RSC Advances

PAPER

Cite this: *RSC Adv.*, 2021, **11**, 27627

Coumarin–carbazole based functionalized pyrazolines: synthesis, characterization, anticancer investigation and molecular docking†

Mrugesh Patel,[a] Nilesh Pandey,*[c] Jignesh Timaniya,[a] Paranjay Parikh,[a] Alex Chauhan,[b] Neeraj Jain*[b] and Kaushal Patel*[a]

Received 21st May 2021
Accepted 27th July 2021

DOI: 10.1039/d1ra03970a

rsc.li/rsc-advances

A series of novel pyrazoline scaffolds from coumarin–carbazole chalcones were synthesized. We explored various acetyl, amide, and phenyl substituents at the *N*-1 position of the pyrazoline core. The synthesized compounds were characterized by FTIR, ^{1}H-NMR, ^{13}C-NMR, DEPT, and mass spectroscopic techniques. The *in vitro* cytotoxicity study of all the synthesized compounds was evaluated against HeLa, NCI-H520 and NRK-52E cell lines. Compounds **4a** and **7b** became the most active compounds and exhibited their potential to arrest the cell cycle progression and induce apoptosis in both the cell lines. In addition, molecular docking studies revealed a higher binding affinity of both the molecules with CDK2 protein. Based on the obtained results, a comprehensive analysis is warranted to establish the role of compounds **4a** and **7b** as promising cancer therapeutic agents.

1. Introduction

Cancer has been one of the major causes of human mortality, and the approximately 10 million deaths in 2020 are predicted to reach up to 16.3 million by 2040.[1] Challenges faced concerning cancer treatment include fatal side effects, low selectivity and solubility, adverse drug interactions, and resistance against varied therapeutic agents. That has led to continual research to identify newer compounds and modify current drugs for safe and effective cancer treatment. In this context, natural products have taken a lead which continues to advance until clinical trials wherein most of the new anticancer drugs are structurally modified/optimized natural compounds.[2] Generally, the natural products are heterocyclic compounds, *i.e.*, they contain heteroatoms in their skeleton that suit well as anticancer drugs either by affecting tubulin polymerization (vincristine and vinblastine) or inhibiting kinase activity (midostaurin), *etc.* However, many of these natural compounds also come with the risk mentioned above. Therefore, there is an exigent need to explore modified natural compound mimics as potential anticancer drug candidates.

Coumarins are naturally occurring oxygen-containing heterocyclic compounds produced by bacteria, fungi, and numerous plant species like Umbelliferae, Asteraceae, Rutaceae, Leguminosae, *etc.*[3,4] Nearly 1300 coumarin derivatives have been identified as secondary metabolites from the same sources. Coumarin compounds have been shown to exert potential anti-microbial, antiviral, anti-tuberculosis, antioxidant, anticancer effects.[5–9] Anticancer properties of coumarin derivative osthole have been potent against hepatocellular carcinoma. The *in vivo* and *in vitro* studies showed that osthole induces apoptosis *via* inhibiting the Akt/NF-κB pathway.[10] A coumarin based drug candidate (RKS262) exerted remarkable potency *in vivo* and *in vitro* on ovarian cancer cell line OVCAR-3.[11] A strategically developed coumarin–monastrol hybrid selectively imparted its anticancer potential over breast cancer cell lines MCF-7 and MDA-MB-231.[12] Coumarin derivatives are used to treat prostate cancer, renal cell carcinoma, and leukemia. They have also been reported to inhibit breast and cervical cancer proliferation and malignant melanoma cell lines.[13]

Like coumarin, carbazole is also a tricyclic nitrogen-containing heterocyclic compound found in various plant species and natural sources. Carbazoles have been shown to possess antibacterial, antifungal, anti-inflammatory, and anticancer activities.[14–17] Carbazole derivative Clausenawalline F revealed potent cytotoxicity on lung cancer cell line NCI-H187.[18] An arylsulfonyl *N*-substituted carbazole derivative exhibited potent inhibition over pancreatic cell lines PANC-1 and Capan-2, and preliminary *in vivo* efficacy studies on mice revealed no

[a]*Department of Advanced Organic Chemistry, P. D. Patel Institute of Applied Sciences, Charotar University of Science and Technology, Gujarat 388421, India. E-mail: kaus_chem@yahoo.com*

[b]*Department of Biological Sciences, P. D. Patel Institute of Applied Sciences, Charotar University of Science and Technology, Gujarat 388421, India. E-mail: neerajjain.as@charusat.ac.in*

[c]*Department of Medical Laboratory Technology, Charotar Institute of Paramedical Sciences, Charotar University of Science and Technology, Gujarat 388421, India. E-mail: nileshpandey.cips@charusat.ac.in*

† Electronic supplementary information (ESI) available. See DOI: 10.1039/d1ra03970a

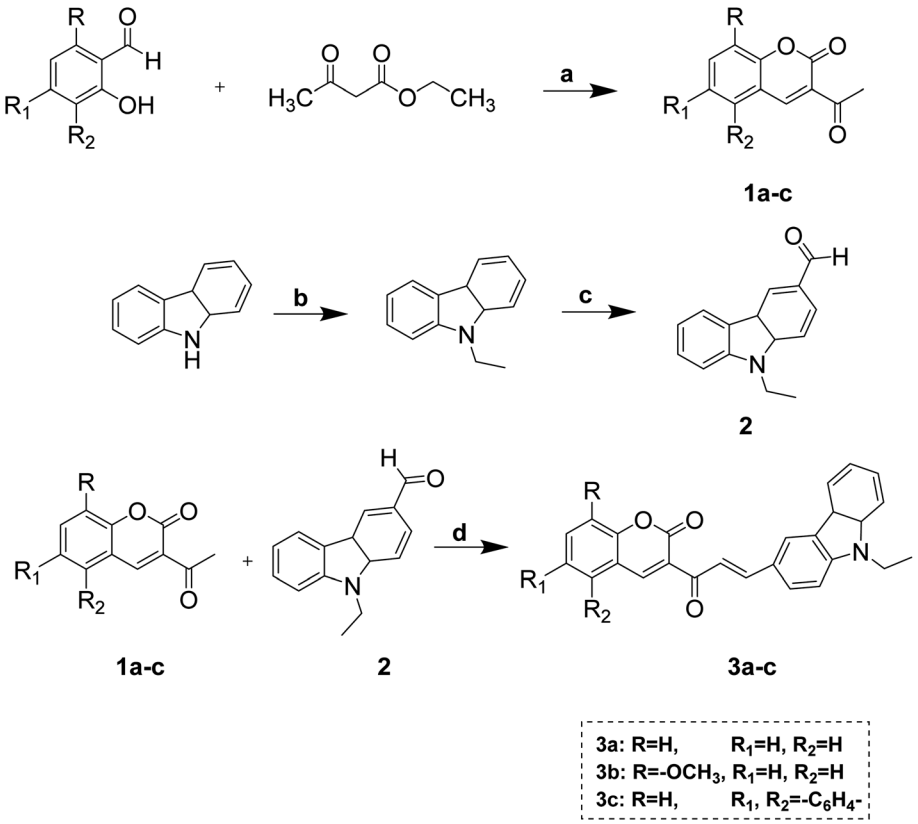

Scheme 1 Synthesis of acetyl-coumarin, formyl-*N*-ethyl carbazole, and coumarin–carbazole chalcone. Reagents and conditions: (a) catalytic amount of piperidine, 70–80 °C, 40 min, (b) C_2H_5Br/KOH, acetone, r.t., (c) DMF/$POCl_3$, (d) catalytic amount of piperidine, ethanol, 65 °C, 2.5–3 h.

side effects.[19] Further, carbazole derivatives Ellipticine, alectinib, and midostaurin are used to treat metastatic breast cancer, ALK-positive advanced non-small-cell lung cancer, and acute myeloid leukemia, respectively, as well as reported to show good cytotoxic activity on various cancer cell lines.[20]

Pyrazoles are another group of heterocyclic compounds from the family of azole group compounds. Azole family members

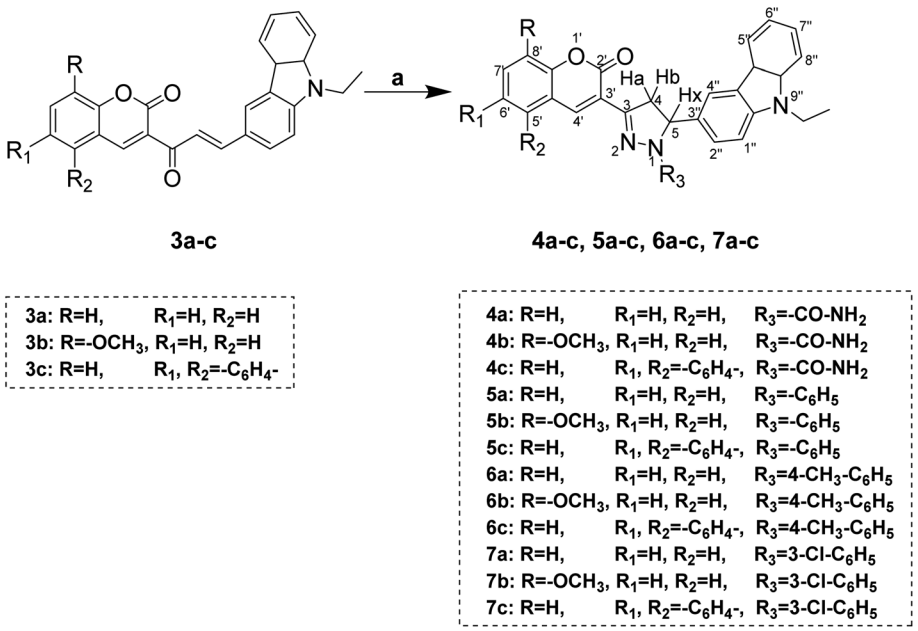

Scheme 2 Synthesis of pyrazoline substituted coumarin–carbazole derivatives. Reagents and conditions: (a) appropriate hydrazine hydrate derivatives, ethanol, a catalytic amount of acetic acid, 65 °C, 1.5–3 h.

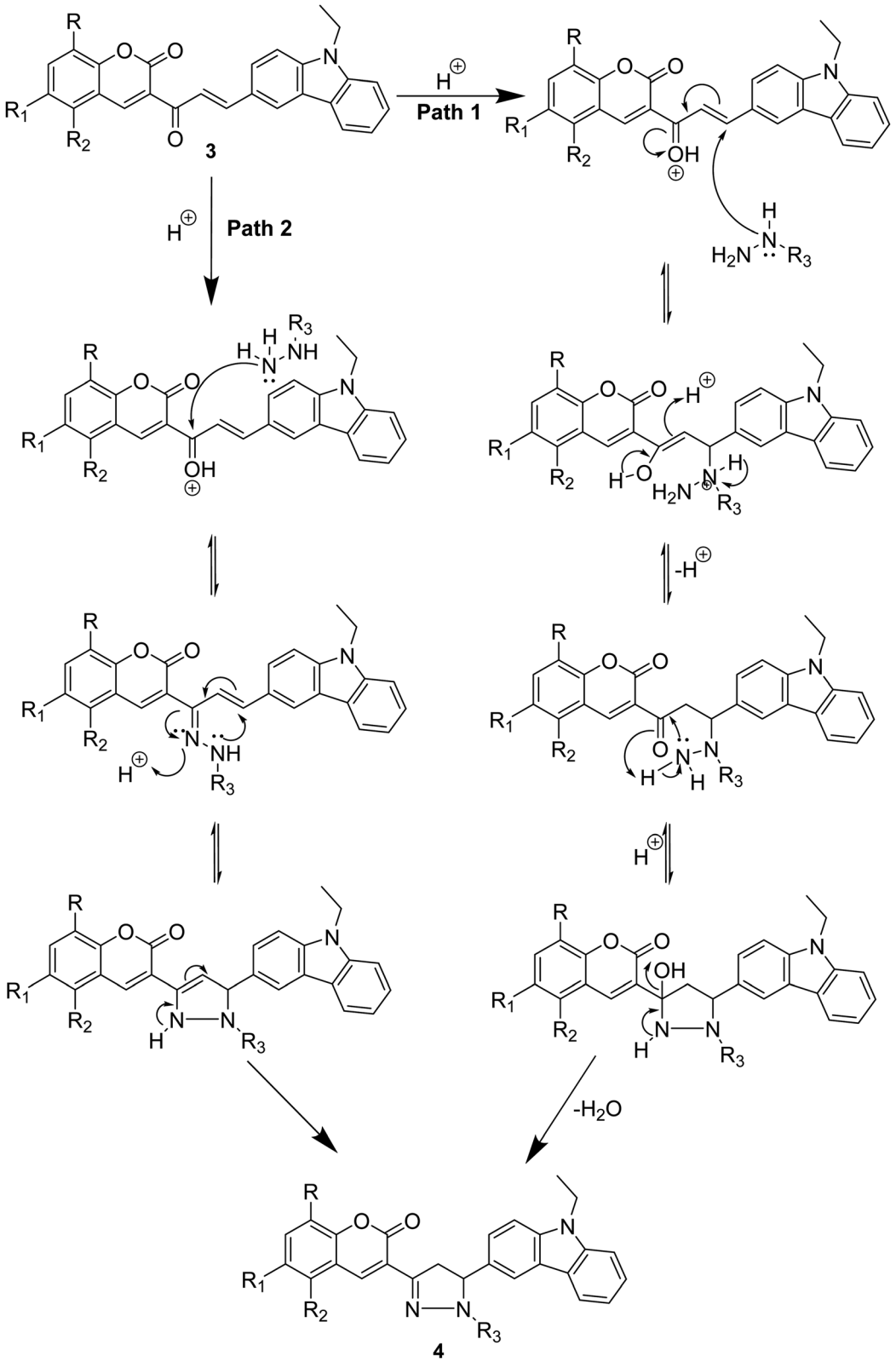

Scheme 3 Plausible reaction mechanism.

possess compounds that contain a nitrogen atom with at least one other hetero atom as part of a five-membered ring, such as thiazoles, oxazoles, *etc.* These compounds contain diverse pharmacological and physiological activities.[21–24] A reduced form of pyrazole, 2-pyrazoline, has been reported to exert potent antimicrobial,[25] anti-inflammatory,[26] anti analgesic,[26]

antioxidant, and anti-cancer[27] activities. Several pyrazole-containing drugs have been serving in clinical trials for years, and many are under current research.[28] One such pyrazole-containing drug candidate, Crizotinib, demonstrated modest multikinase inhibitory activity in non-small-cell lung carcinoma patients harboring MET exon 14 mutation[29] and exhibited antitumor activity in advanced non-small-cell lung cancer patients with ROS1-rearrangement.[30] For patients with ALK-positive non-small-cell lung cancer. Similarly, in non-small-cell lung cancer patients with *ALK* mutations, another pyrazole-containing drug candidate, Lorlatinib, showed anti-tumor activity in the global phase II trial.[31] Additionally, phase I and II study of Zanubrutinib, a pyrazole consisting of drug candidates, revealed anticancer activity in mantle cell lymphoma, a multikinase inhibitor.[32] Moreover, pyrazole-containing drug Pazopanib is known to inhibit angiogenesis by blocking tyrosine kinase activity.[33] Thus, most coumarin, carbazole, and pyrazole derivatives impart their cytotoxicity *via* inhibiting kinases that are vital drug target molecules in cancer therapy.

In terms of clinical efficacy, conventional single-target therapy has revealed pharmacokinetic limitations leading to insufficient control on malignancy. Nonetheless, these limitations have opened the gates of research on multi-target hybrid drug therapy to effectively kill cancer cells with minimal side effects. The hybridization of two or more moieties in a single molecule provides a potent hybrid pharmacophore to develop newer anticancer compounds.[34]

Considering this fact, we merged three potential pharmacophores, coumarin, carbazole, and pyrazole, into one compound to augment the individual molecule's potential for anticancer activity. The merger of two pharmacophores was performed by making chalcone of two moieties. Although there are many ways by which the merger of two pharmacophores is possible but making chalcone of both the moieties is one of the efficient and more applicable methods for the conjunction of coumarin and carbazole by reacting with appropriate hydrazines in ethanol using a catalytic amount of acetic acid.

In the present study, **4a–c**, **5a–c**, **6a–c**, **7a–c**, and **8a–c** compounds were investigated for cytotoxicity followed by cell cycle and apoptotic analysis in cancer cell lines HeLa and NCI-H520 to assess anticancer activities. Furthermore, *in silico* molecular docking, it was carried out to predict binding affinity between active compounds and cyclin-dependent kinase 2 (CDK2).

2. Results and discussion

2.1. Chemistry

The target compounds (**3a–c**) were obtained using the synthetic procedure and the substitution pattern depicted in Scheme 1. The first precursor's acetyl derivatives of coumarins were

Table 1 Cytotoxicity of the compounds (**3a–8c**) evaluated on HeLa, NCI-H520, and NRK-52E cell lines

	IC_{50}, μM		
Compounds	HeLa	NCI–H520	NRK-52E
3a	131.6 ± 5.16	119.86 ± 3.78	94.60 ± 3.97
3b	118.7 ± 6.88	103.24 ± 4.78	115.30 ± 7.23
3c	141.8 ± 7.77	132.66 ± 4.75	82.67 ± 1.87
4a	12.59 ± 0.10	11.26 ± 0.45	28.37 ± 1.29
4b	29.82 ± 1.85	22.48 ± 2.15	40.32 ± 1.92
4c	43.48 ± 1.02	55.61 ± 1.93	59.05 ± 0.91
5a	92.50 ± 4.25	81.24 ± 1.46	102.96 ± 1.65
5b	39.03 ± 0.46	62.70 ± 1.63	70.35 ± 3.68
5c	55.00 ± 0.96	83.57 ± 1.20	121.70 ± 7.03
6a	67.03 ± 1.87	38.31 ± 0.78	83.24 ± 5.14
6b	30.80 ± 0.50	30.01 ± 0.33	51.99 ± 4.27
6c	57.51 ± 1.32	61.67 ± 1.48	79.92 ± 5.10
7a	33.44 ± 0.64	14.31 ± 0.21	40.98 ± 3.80
7b	11.36 ± 0.24	9.13 ± 0.08	24.16 ± 1.73
7c	29.04 ± 0.84	20.83 ± 0.27	57.11 ± 3.59
8a	43.18 ± 0.52	62.46 ± 1.95	116.26 ± 6.95
8b	76.78 ± 1.45	54.72 ± 0.65	97.92 ± 4.99
8c	55.85 ± 1.30	77.61 ± 0.34	81.27 ± 3.77
Cis-platin	7.75 ± 0.42	10.41 ± 1.35	12.93 ± 0.40
5-Fluorouracil	55.72 ± 2.10	8.36 ± 0.45	46.68 ± 3.79

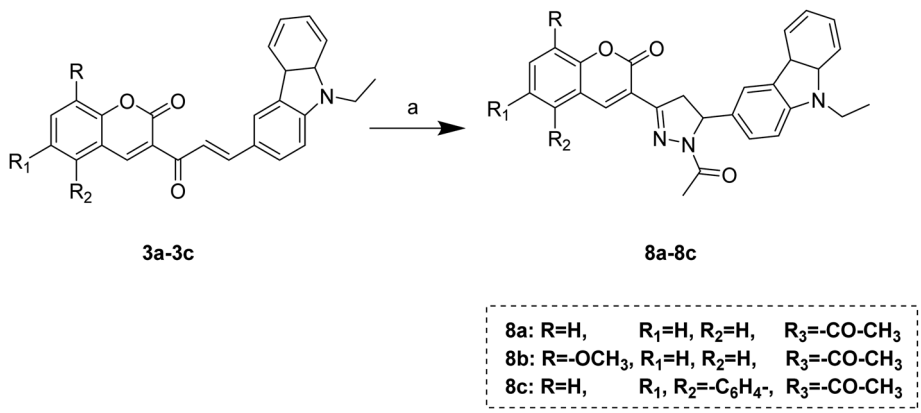

Scheme 4 Synthesis of *N*-acetyl pyrazoline substituted coumarin–carbazole derivatives. Reagents and conditions: (a) hydrazine hydrate, acetic acid, ethanol, 65 °C, 1.5–3 h.

synthesized according to the reported procedure,[35,36] and 9-ethyl-9*H*-carbazole-3-carbaldehyde was synthesized by initial ethylation of carbazole by the reaction of bromoethane and potassium hydroxide in acetone; the ethylated product was formulated using Vilsmeier–Haack reaction.[37] Both the precursor further consumed for the synthesis of chalcone.

Coumarin–carbazole chalcones (**3a–c**) were obtained by reacting 3-acetyl coumarins derivatives, 6-formyl carbazole, and piperidine in ethanol. Pyrazoline derivatives (**4a–c**, **5a–c**, **6a–c**, **7a–c**) were obtained by reacting chalcone (**3a–c**) with appropriate hydrazines in ethanol using a catalytic amount of acetic acid shown in Scheme 2.

The plausible mechanism for pyrazolines synthesis is illustrated in Scheme 3. The mechanism proceeded in two ways: path 1 involved an initial attack of nucleophilic secondary amine-nitrogen of substituted hydrazine on the carbon–carbon double bond of chalcone to form an intermediate underwent cyclization and rearrangement to afford pyrazoline. Path 2 involved an initial attack of nucleophilic terminal nitrogen of substituted hydrazine on the carbonyl carbon to form an intermediate that underwent a second nucleophilic attack of imine nitrogen resulting in cyclization and after rearrangement afforded a pyrazoline ring.

However, acetyl derivatives of pyrazolines (**8a–c**) were obtained by reacting chalcones (**3a–c**), hydrazine hydrate, acetic acid in ethanol shown in Scheme 4.

In this study, the Claisen–Schmidt condensation was preferred for the synthesis of chalcones, and these chalcone derivatives were further reacted with hydrazines to obtain the final targeted pyrazolines. The purity of compounds was established by thin-layer chromatography (TLC), and purification was performed using column chromatography.

2.2. Characterization

All the synthesized compounds were characterized using spectral techniques such as IR, ^{1}H NMR, ^{13}C NMR, DEPT, MS, and elemental analysis. The compounds were then tested for their cytotoxicity over cancer cell lines HeLa and NCI-H520, and normal cell lines NRK-52E. The best performing hybrids were further investigated for cell cycle progress, apoptosis-inducing effects, morphological changes, and molecular docking studies.

The spectral analysis data confirmed the synthesized compounds **3a–3c**, **4a–4c**, **5a–5c**, **6a–6c**, **7a–7c** and **8a–8c**. The ring closure reaction of chalcones established the FTIR spectra of final pyrazoline compounds. Infrared spectra revealed two characteristic bands absorption for N–H stretching between

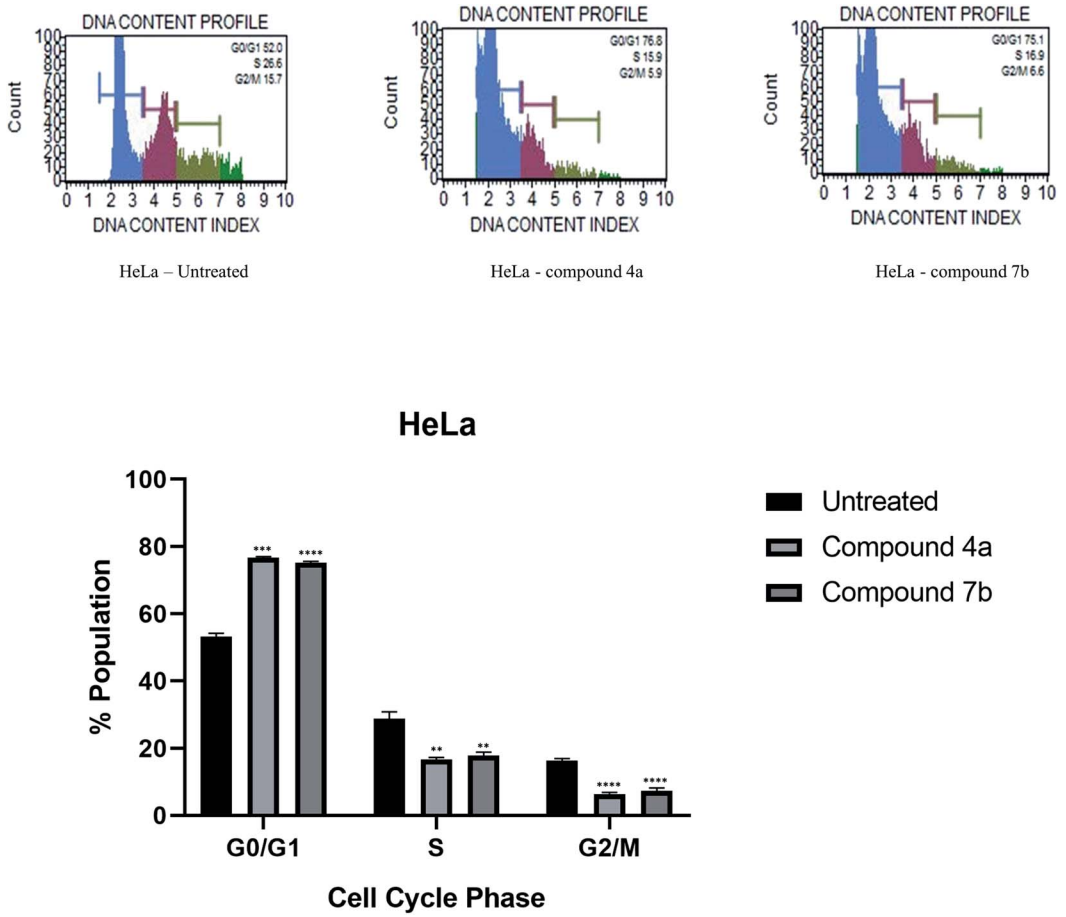

Fig. 1 Effect of compounds **4a** and **7b** on the cell cycle of cervical cancer cells HeLa and its graphical presentation. Data are represented mean ± SE. $p < 0.05$ was considered statistically significant compared to the untreated cells.

3200–3500 cm^{-1}. Absorption around 1729 cm^{-1} related to C=O stretching of δ-lactone of coumarin and absorption between 1600–1680 cm^{-1} was observed due to stretching of C=O of chalcone, amide, and acetyl functional groups of molecules; the band appears for carbonyl of chalcone in this region disappears after the formation of pyrazoline from chalcone which can be seen in pyrazolines which do not possess acetyl and amide functionalities. Stretching bands appear between 1592–1628 cm^{-1} indicates the conversion of chalcone to pyrazoline as C=N bond formation. Chalcone **3a** showed bands in infrared region at 3072 cm^{-1} for aromatic C–H stretching, 2972, 2929 & 2868 cm^{-1} for aliphatic C–H stretching, 1729 cm^{-1} for C=O stretching of δ-lactone of coumarin, 1677 cm^{-1} for C=O stretching of chalcone, 1569 & 1470 cm^{-1} for C=C stretching. Pyrazoline compound **4a** showed bands at 1730 and 1666 cm^{-1} for C=O of coumarin carbonyl and amide carbonyl, respectively. The band at 1605 cm^{-1} corresponds to –C=N confirms the formation of –C=N bond and the pyrazine –C=N– bonds, while the bands at 1572 and 1467 cm^{-1} are due to the –C=C– bond. The bands at 1133 to 1231 cm^{-1} were qualified to the (–C–N) vibrations, confirming the pyrazoline ring cyclization in all compounds. A band at 3344 and 3297 cm^{-1} owing to $–NH_2$ of amide derivative was observed.

^{1}H NMR resonance of compounds **3a–c**, **4a–c**, **5a–c**, **6a–c**, **7a–c**, and **8a–c** showed the signal for aliphatic protons of *N*-ethyl carbazole that appeared between 1.29–1.48 δ ppm for $–CH_3$ as a triplet and 4.31–4.41 δ ppm for $–CH_2$ as a quartet. The $–CH_2$ protons of the pyrazoline ring resonated as a pair of a doublet at 3.38–3.57 (Ha) δ ppm and 3.98–4.25 (Hb) δ ppm. The –CH proton of the pyrazoline ring appeared as a doublet of doublets at 5.50–5.78 (Hx) δ ppm due to vicinal coupling to non-equivalent protons Ha and Hb. In compounds **4a–4c**, a broad singlet was observed between 5.40–6.72 δ ppm due to N–H protons of amide-functionality of the pyrazoline ring. Similarly, in compounds **8a–8c**, a singlet was observed between 2.34–2.44 δ ppm for $–CH_3$ of acetyl derivatives. All the aromatic protons gave a signal between 6.74–9.49 δ ppm. ^{1}H NMR spectra confirmed the structures of chalcones **3a–3c**. In compound **3a**, a peak at 1.45 δ ppm appeared as a triplet for $–CH_3$ of $N–CH_2–C\mathbf{H_3}$, and a peak at 4.37 ppm appeared as a quartet for $–CH_2–$ of $N–C\mathbf{H_2}–CH_3$. The multiplet was observed between 7.26–7.99 δ ppm, a triplet for two aromatic protons observed at 8.12 ppm, a doublet appeared for one proton at 8.38 ppm, and a singlet appeared for one proton at 8.58 ppm for aromatic proton. The ^{1}H NMR spectra of compound **4a** showed a pattern of protons of the pyrazoline ring caused by the three hydrogen atoms coupling (Ha, Hb and Hx) 2-pyrazoline ring at 3.50 ppm, dd 4.05 ppm, and dd 5.73 ppm, respectively. The existence of methylene protons (Ha and Hb) as a doublet of doublets postulates the magnetic non-equivalence of these two protons. The alkyl protons ($–CH_3$ and $–CH_2$) appear at the downfield at 1.40 ppm and 4.33 ppm due to carbazole's nitrogen deshielding effect. The two-broad singlet of NH_2 group proton for

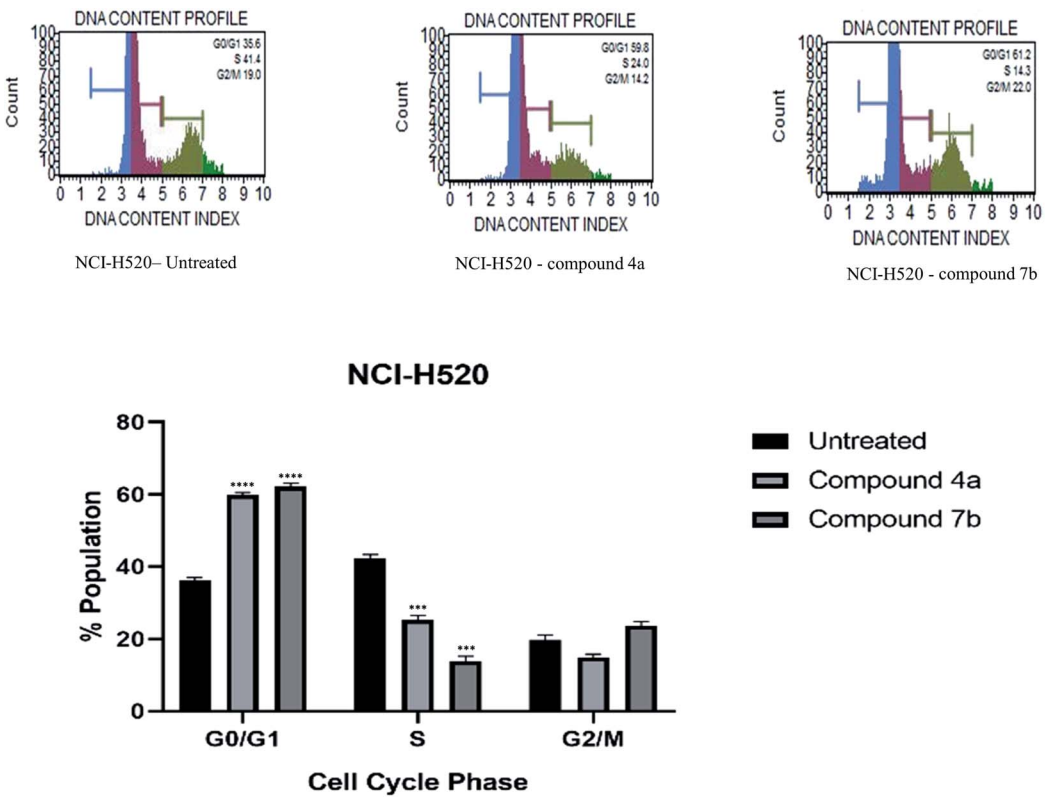

Fig. 2 Effect of compounds **4a** and **7b** on the cell cycle of lung cancer cells NCI-H520 and its graphical presentation. Data are represented mean ± SE. $p < 0.05$ was considered statistically significant compared to the untreated cells.

compound **4a** was observed at 5.40 ppm. These spectral data unequivocally proved the 2-pyrazoline structure.

^{13}C NMR spectra of all the synthesized pyrazolines showed all carbonyl group signals between 157.63–159.85 δ ppm. The carbonyl of chalcone appears around 186 δ ppm, generally disappears after generation of pyrazoline ring over chalcone functionality. All the aromatic carbons appeared between 108.37–155.88 δ ppm. The ^{13}C NMR spectra of the compounds provided the final carbon skeleton of pyrazolines. The value of the chemical shift of (–CH_3) of carbazole carbons appears around 13.79 ppm, while in (–CH_2) of carbazole appears around 45.21 ppm. The chemical shifts around 37.52 ppm, 61.03 ppm are due to (–CH_2) and (–CHx) of carbons to the pyrazoline; it was observed that CHx signals generally appears around 60 ppm, but in the case of compounds **5a–c**, **6a–c**, **7a–c** due to the presence of pendant phenyl ring that signal shifts towards 65 ppm. The ^{13}C NMR spectra of chalcone **3a** give chemical shift of (–CH_3) of carbazole carbons appears at 13.85 ppm, while in (–CH_2) of carbazole appears at 37.81 ppm. The aromatic ring carbons of compound **3a** appear in their desired aromatic region 108–147.56 δ ppm. The peaks at 186.20 ppm and 159.46 ppm are of the C=O of chalcone and C=O of coumarin carbons. The aromatic ring carbons of pyrazoline derivative **4a** appear in their desired aromatic region. The peaks at 158.85 ppm and 155.18 ppm are of the C=O of coumarin and C=O of amide carbons. Mass spectral analysis of compounds indicated peaks concerning the molecular weight of compounds.

2.3. Biology

2.3.1. Cytotoxicity effect. *In vitro* cytotoxic activity of synthesized compounds was performed using MTT assay on cancer cell lines HeLa and NCI-H520 and normal rat kidney epithelial cell line NRK-52E. The IC_{50} value representing the compound's inhibitory concentration causing 50% cell population death was calculated based on the dose–response curve generated after obtaining percent cell death at different concentrations of the compound. The results obtained were compared with the reference drugs cis-platin and 5-fluorouracil under similar experimental conditions.

Cytotoxicity was expressed as the mean IC_{50} of three independent experiments (Table 1). All the synthesized compounds exhibited cytotoxicity with IC_{50} values in the range of 9.13–141.8 μM. The majority of synthesized compounds were less active on NRK-52E than the other two cancer cell lines. The chalcone derivatives **3a–3c** exhibited low inhibition over all the cell lines as compared to pyrazolines. Two of the all pyrazoline scaffolds, *N*-amide pyrazoline **4a** and *m*-chloro substituted *N*-phenyl pyrazoline **7b**, exhibited remarkable IC_{50} at 12.59, 11.36 μM respectively against HeLa and 11.26, 9.13 μM respectively against NCI-H520. Compound **7b** also exhibits an IC_{50} of 24.16

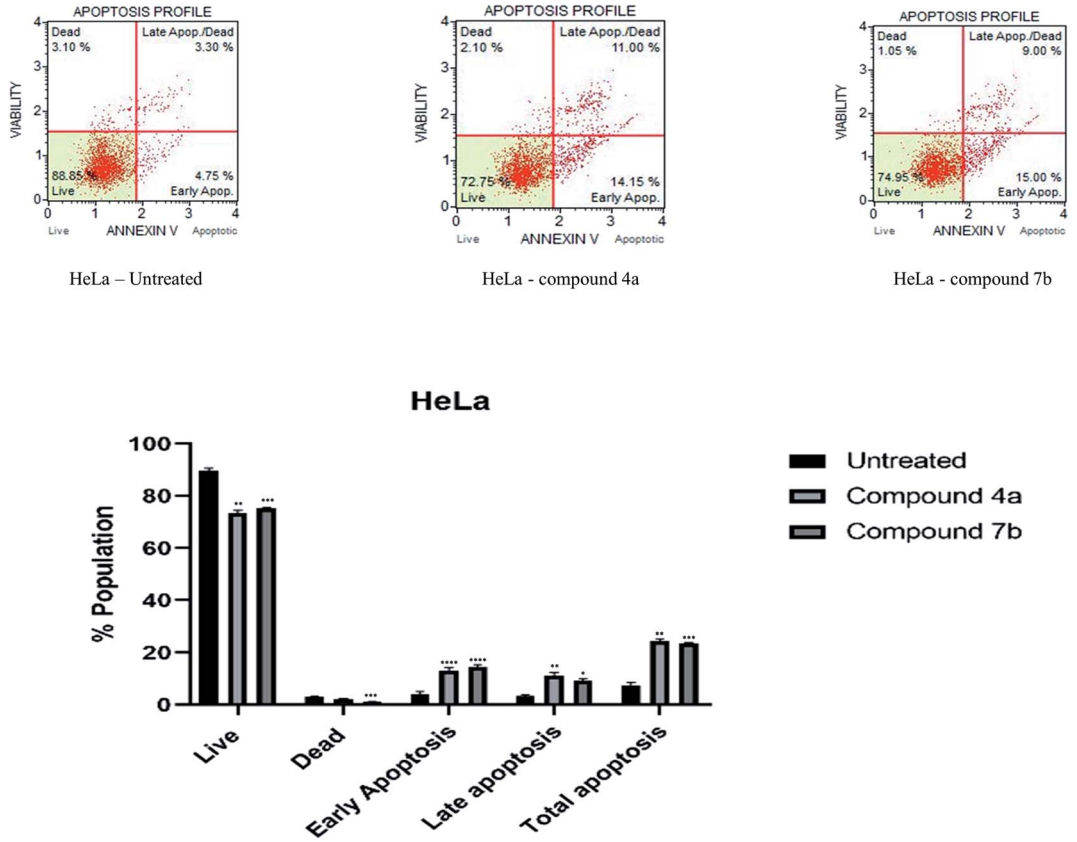

Fig. 3 Apoptosis of HeLa cells induced by compounds **4a** and **7b** and its graphical presentation. Data are represented mean ± SE. $p < 0.05$ is considered statistically significant compared to the untreated cells.

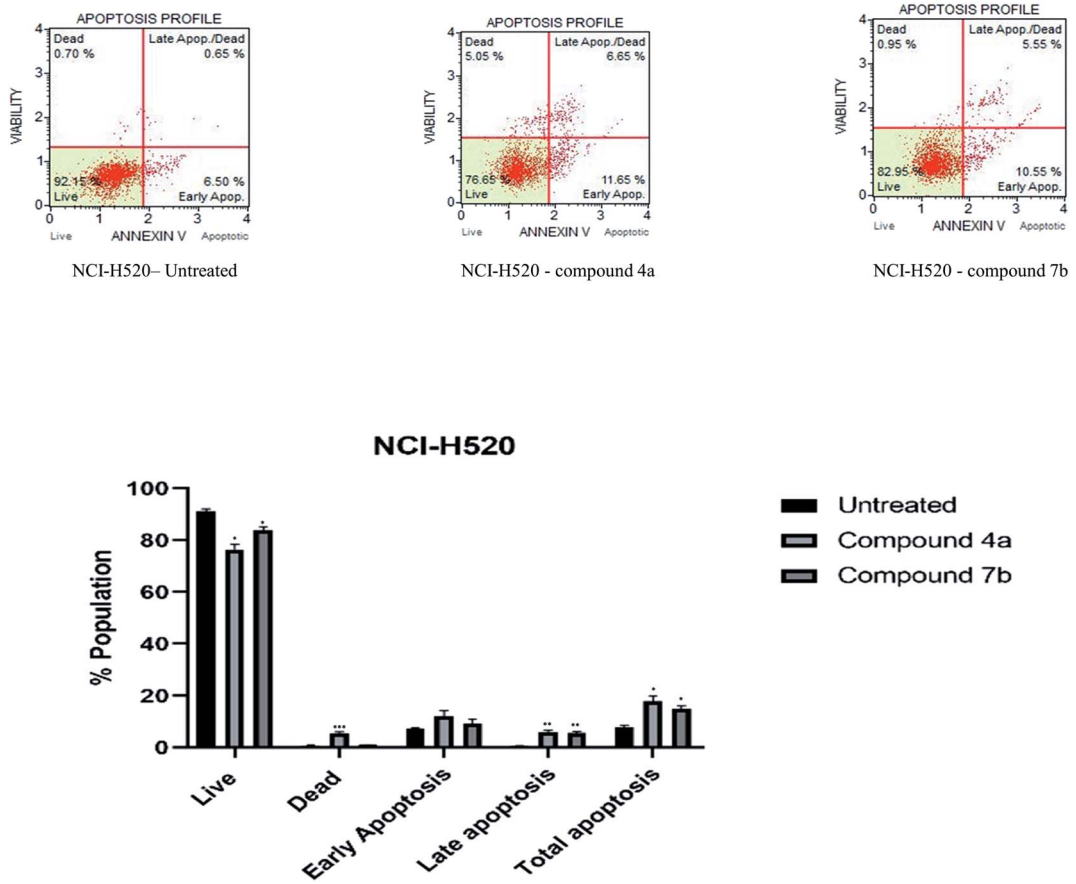

Fig. 4 Apoptosis of NCI-H520 cells induced by compounds **4a** and **7b** and its graphical presentation. Data are represented mean ± SE. $p < 0.05$ is considered statistically significant compared to the untreated cells.

μM over NRK-52E cell lines. Compounds **4b** and **7c**, which contained a methoxy group on the 8th position of coumarin, showed good activity against HeLa at 29.82, 29.04 μM, respectively, and NCI-H520 22.48, 20.83 μM concentrations, respectively. The rest of the compounds exhibited moderate to low activity on all three cell lines.

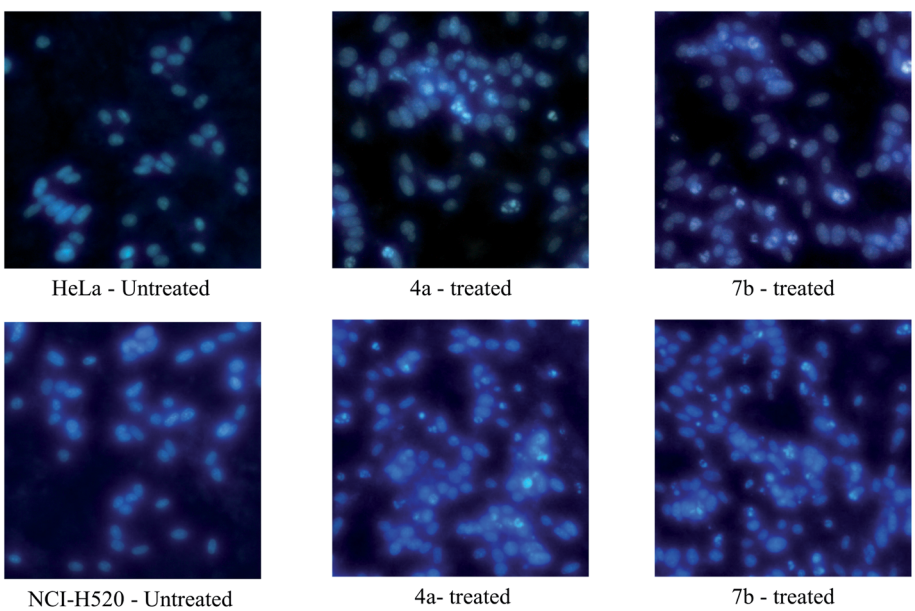

Fig. 5 Nuclear morphologic changes were observed after 24 h treatment of compounds **4a** and **7b** on HeLa and NCI-H520 cells.

2.3.2. Cell cycle analysis. The two most potent compounds **4a** and **7b**, based on their high inhibitory activity, were selected to study their effect on cell cycle distribution in HeLa and NCI-H520. Both the compounds triggered cells' accumulation in the G0/G1 phase compared to untreated control (Fig. 1). The HeLa cell population in the G0/G1 phase increased to 76.8% and 75.1% (Fig. 1), whereas NCI-H520 cells increased to 59.8% and 61.2% (Fig. 2) after 24 h treatment with compounds **4a** and **7b**, respectively, compared to their untreated 52.0% (Fig. 1) and 35.6% (Fig. 2) cells respectively. A graphical representation of the same is depicted in Fig. 2. The results showed a statistically significant difference in the G0/G1 cell population of both HeLa

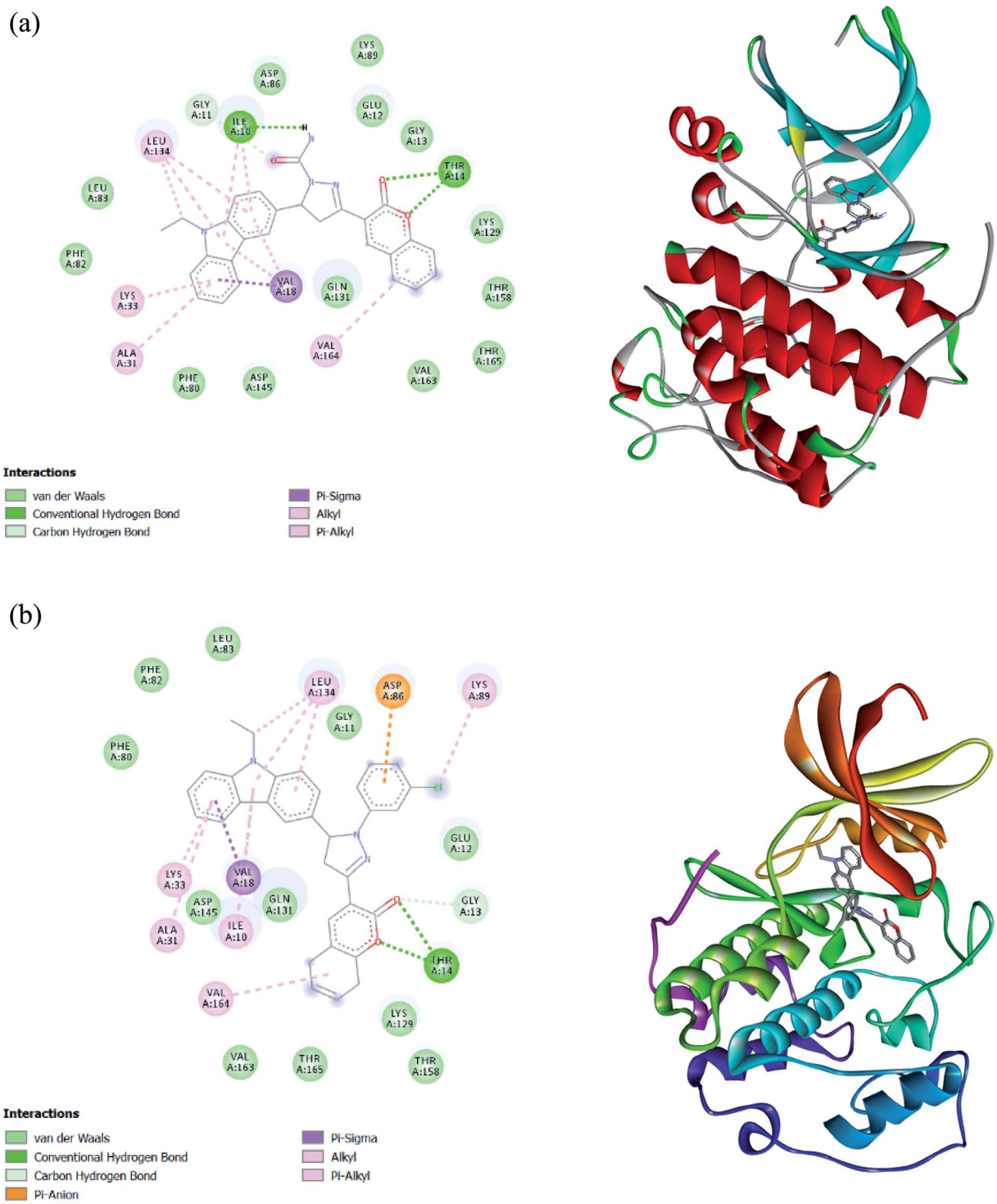

Fig. 6 (a) *In silico* docking model of CDK2 protein with the ligand, **4a** shows 2D and 3D images generated with Biovia Discovery Studio Visualizer. (b) *In silico* docking model of CDK2 protein with the ligand, **7b** shows 2D and 3D images generated by Biovia Discovery Studio Visualizer.

(***$p < 0.001$) and NCI-H520 cells (****$p < 0.0001$) compared to untreated cells.

2.3.3. Apoptosis study. Increased number of cells in the G0/G1 phase after treatment with coumarin–carbazole based pyrazoline hybrids indicated their role in inducing apoptosis. Therefore, the apoptotic effect of compounds **4a** and **7b** was carried out using Muse Annexin V & Dead cell kit. HeLa cells treated with compounds **4a** and **7b** at their IC50 dose of 12.59 μM and 11.26 μM respectively, for 24 h, displayed a significant 25.5% and 24% increase in apoptotic cells, respectively, compared to 8.05% of untreated cells (**$p < 0.005$) (Fig. 3). Similarly, the treatment of NCI-H520 cells with IC_{50} dose of compound **4a** and **7b** revealed an 18% and 16.10% increase in apoptotic cell death, respectively, compared to 7.15% untreated cells (*$p < 0.05$) (Fig. 4). Furthermore, both HeLa (*$p < 0.05$) and NCI-H520 (**$p < 0.005$) showed a statistically significant increase in the proportion of late apoptotic cells compared to untreated controls. Compound **4a** (****$p < 0.0001$) and **7b** (****$p < 0.0001$) also displayed a significant effect in the increase of early apoptotic HeLa cells, however; no such significant effect was observed on NCI-H520 cells with regards to early apoptosis. The results obtained revealed a vital role of compounds **4a** and **7b** in programmed cell death.

2.3.4. Detection of nuclear morphological changes. To further assure the apoptotic potential of compounds **4a** and **7b**, we looked into DNA condensation and fragmentation, which are vital indicators of cells undergoing apoptosis. The cells were treated with DAPI, a cell-permeable fluorescence dye that strongly binds to A–T-rich regions of DNA and aids in analyzing nuclear condensation and fragmentation.[38] A 24 h treatment of the compounds **4a** and **7b** at their respective IC_{50} dose on HeLa and NCI-H520 cells revealed condensed and fragmented nuclei compared to intact nuclear bodies of untreated cells (Fig. 5).

2.3.5. Molecular docking analysis. The induction of cell cycle arrest in the G0/G1 phase and increased apoptosis due to the effect of compounds **4a** and **7b** encouraged us to explore the probable mechanism by which these molecules might be operating by determining their theoretical binding site and the binding energies with CDK2 as is a crucial regulator of the cell cycle at the early and late G1 phase along with cyclin A and cyclin D,[39] which hinders cells programmed death and plays a significant role in tumorigenesis.[40]

2.3.5.1. Interaction with CDK2. The docking analysis revealed a higher binding affinity −11.5 kcal mol^{-1} and −11.9 kcal mol^{-1} of molecules **4a** and **7b**, respectively, at the active site of CDK2. The interaction was compared with the roscovitine (PDB ID: 2A4L). Concerning **4a**, Ile10 of CDK2 formed a hydrogen bond (2.58 Å) with the amide group. A novel hydrogen bonding was observed where Thr14 of CDK2 was involved in two hydrogen bonds (3.08 Å, 2.38 Å) with the two oxygen present in the coumarin ring. The other bonds showing bond length between 3 and 4 Å in the interaction were (i) a pi-alkyl bond (3.90 Å) between Val18 and the aromatic ring of carbazole and (ii) the carbon–hydrogen bond (3.35 Å) between Gly11 and oxygen of an amide linkage. Several common amino acids such as Leu134, Lys33, Leu83, Phe80, Asp145, and Lys89 also showed interaction with **4a** (Fig. 6a); however, the interaction type was not similar to standard roscovitine.[41] The analysis of **7b** interaction with CDK2 also revealed the formation of two hydrogen bonds (2.65 Å, 2.28 Å). The other interactions with ≈4 Å bond length were: Pi anion (3.96 Å) between Asp86 and substituted phenyl ring of pyrazoline, Pi sigma (3.91) formation of Val18 with the aromatic ring of carbazole, carbon–hydrogen bond (3.21 Å) between Gly13 and oxygen of carbonyl of coumarin, Leu134 forming Pi-alkyl bond (4.01 Å) with pendant methylene of carbazole attached with nitrogen, Lys89 forming pi-alkyl bond (4.04 Å) with chlorine of substituted pyrazoline of phenyl and Met115 forming pi alkyl bond (4.2 Å) with lactone ring of coumarin. Comparing the binding of **7b** with PDB ID: 2A4L following interacting amino acids Tyr108, Ala149, Val156, Phe112, Leu137, and Asp111 (Fig. 6b) were detected to be common. An additional hydrogen bond was formed with the Thr14 at the active site signifying its potential inhibitor. The interaction of **4a** and **7b** with the active site of CDK2 depict its potential as an inhibitor, which needs to be validated through laboratory experimentation.

2.3.6. Structural activity relationship (SAR). The biological evaluation findings showed that the response was significantly affected by substituting separate functional groups in the pyrazoline ring at the R_3 position and coumarin ring at the R, R_1, and R_2 positions. The amide group's introduction at the R_3 position increased cytotoxicity against HeLa and NCI-H520 cells. The amide group at R_3 position of pyrazoline with a methoxy group at R position of coumarin possesses moderate

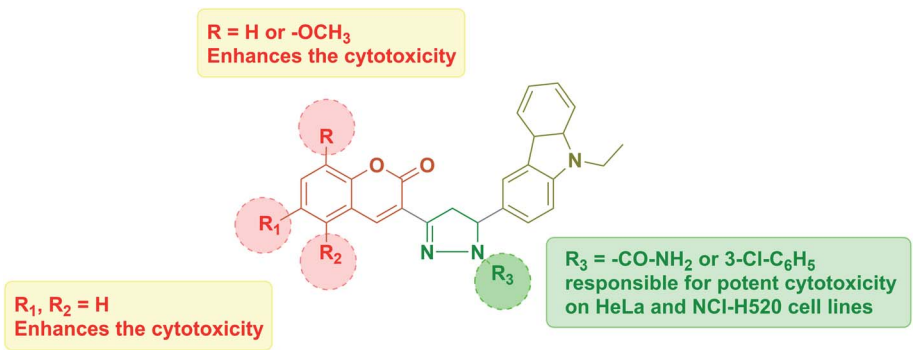

Fig. 7 Structural activity relationship (SAR).

Table 2 Grid centers for docking analysis

Protein	Centre X (Å)	Centre Y (Å)	Centre Z (Å)
2A4L	100.865	101.747	79.893
6QGG	−15.226	14.319	−9.635

activity and significantly less activity observed for benzo-fusion in coumarin at R_1–R_2 position against both the cell lines. Although the acetyl group containing all the three compounds were low to moderately active against both the cell lines, substitution of phenyl group over R_3 position of pyrazoline having different substituents, *i.e.*, a methyl group and chloro group present at the fourth and third position respectively on phenyl ring was responsible for the significant activity. Particularly chloro substitution in the phenyl group enhanced the cytotoxicity against both the cell lines. Out of three chlorophenyl substitutions containing hybrids, the one with methoxy substitution attached to coumarin was observed high potency amongst all the synthesized derivatives against HeLa and NCI-H520 cells. In contrast, the phenyl group with a methyl group at the fourth and non-substituted phenyl groups was low to moderately active observed on both the cell lines (Fig. 7).

3. Conclusion

In summary, this investigation represents an efficient mild conditioned route for the synthesis of novel coumarin–carbazole containing pyrazoline derivatives. This final hybrid structure includes many pharmacophores in single molecules that may result in varied structural diversity. Compounds **4a** and **7b** possessing *N*-amide pyrazoline and *m*-chloro substituted *N*-phenyl pyrazoline were most potent against cancer cell lines HeLa and NCI-H520, whereas moderately active on normal rat epithelial NRK-52E cell line. The excellent cytotoxic potency of both the compounds was also investigated and found to potentially arrest the cell cycle phase in the G0/G1 phase and induce apoptosis in both the cell lines. The molecular docking study of both the potent candidates on CDK2 rationalized their inhibition with high docking score. We expect these active functions to endow molecules to contribute to the broader range of applications. This study provides valuable information for structurally designing and developing potent coumarin hybrids as promising cancer therapeutic agents.

4. Materials and methods

4.1. Chemistry

Reagents and solvents were obtained from commercial sources and used without further purification. All melting points were determined by using Precision Digital Melting/Boiling Point Apparatus by VEEGO (Model: Vmp-D/Ds). Thin-layer chromatography (TLC, aluminium plates coated with silica gel 60 F_{254}, 0.25 mm thickness, Merck) was used for monitoring the progress of all reactions, purity, and homogeneity of the synthesized compounds. FT-IR spectra were recorded using potassium bromide disc on Nicolet 6700 FT-IR spectrophotometer, and only the characteristic peaks are reported. Elemental analysis was carried out on Perkin-Elmer 2400 Series II CHNS/O Analyzer. In addition, ^{1}H-NMR and ^{13}C-NMR spectra were recorded using DMSO-d_6 and $CDCl_3$ as a solvent on a Bruker Avance spectrometer at a 400 MHz frequency 100 MHz, respectively, using TMS as an internal standard. The splitting pattern of NMR signals is as singlet (s), doublet (d), doublet of doublets (dd), doublet of doublets of doublets (ddd), triplet (t), quartet (q), multiplet (m). The coupling constant (J) is given in Hertz (Hz). Mass spectra were documented on Shimadzu QP2010 Spectrometer.

4.1.1. Synthetic procedures and spectral data

*4.1.1.1. General synthetic procedure for compounds **3a–c**.* A mixture of 6-formyl, 9-ethyl carbazole (**2**) (3 mmol), various 3-acetyl coumarin (**1a–c**) (3 mmol), and piperidine (0.3 mmol) in 30 mL of ethanol was stirred at 70 °C for 45–60 min. Then, the mixture was filtered, and the precipitated chalcone product was washed with cold ethanol.

*4.1.1.2. (E)-3-(3-(9-Ethyl-9H-carbazol-3-yl)acryloyl)-2H-chromen-2-one (**3a**).* Yield: 85%; mp 194–196 °C (lit[42]); yellow solid; IR spectrum, ν_{max}, cm^{-1}: 3072 (aromatic C–H stretching), 2972, 2929 and 2868 (aliphatic C–H stretching), 1729 (C=O stretching of δ-lactone of coumarin), 1677 (C=O stretching of chalcone), 1569 & 1470 (C=C); ^{1}H NMR ($CDCl_3$) δ, ppm (J, Hz): 1.45 (3H, t, J = 7.2 Hz, CH_3 of carbazole), 4.37 (2H, q, J = 7.2 Hz, CH_2 of carbazole), 7.29 (1H, t, J = 7.2 Hz, Ar-H), 7.33 (1H, t, J = 7.6 Hz, Ar-H), 7.40 (3H, t, J = 7.2 Hz, Ar-H), 7.49 (1H, t, J = 7.2 Hz, Ar-H), 7.61–7.66 (2H, m, Ar-H), 7.83 (1H, dd, J = 1.6 Hz and 7.2 Hz, Ar-H), 7.96–7.99 (1H, m, Ar-H), 8.12 (2H, t, J = 8.0 Hz, Ar-H), 8.38 (1H, d, J = 1.2 Hz, Ar-H), 8.58 (1H, s, Ar-H); ^{13}C NMR ($CDCl_3$): δ (ppm) 186.20(C=O of chalcone), 159.46(C=O of coumarin), 155.17(C), 147.56(Ar-CH), 147.05(AR-CH), 141.76(C), 140.49(C), 133.92(CH), 129.91(CH), 126.88(CH), 126.35(CH), 125.96(C), 125.85(C), 124.88(CH), 123.50(C), 122.93(C), 122.43(CH), 120.87(CH), 120.75(CH), 119.83(CH), 118.72(C), 116.66(CH), 108.91(CH), 37.81(CH_2 of carbazole), 13.85(CH_3 of carbazole). Anal. calcd for $C_{26}H_{19}NO_3$: elemental analysis: C, 79.37; H, 4.87; N, 3.56%. Found: C, 79.39; H, 4.86; N, 3.52%.

*4.1.1.3. (E)-3-(3-(9-Ethyl-9H-carbazol-3-yl)acryloyl)-8-methoxy-2H-chromen-2-one (**3b**).* Yield: 82%; mp 245–246 °C (lit[42]); yellow solid; IR spectrum, ν_{max}, cm^{-1}: 3056 (aromatic C–H stretching), 2971, 2929 & 2838 (aliphatic C–H stretching), 1729 (C=O stretching of δ-lactone of coumarin), 1651 (C=O stretching of chalcone), 1573 & 1471 (C=C); ^{1}H NMR ($CDCl_3$) δ, ppm (J, Hz): 1.46 (3H, t, J = 7.2 Hz, CH_3 of carbazole), 4.38 (2H, q, J = 7.2 Hz, CH_2 of carbazole), 4.0 (3H, s, –OCH_3 of coumarin), 7.17 (1H, dd, J = 7.2 Hz and 2.0 Hz, Ar-H), 7.23–7.30 (3H, m, Ar-H), 7.42 (2H, dd, J = 8.0 Hz and 2.8 Hz), 7.50 (1H, t, J = 7.2 Hz, Ar-H), 7.84 (1H, dd, J = 7.2 Hz and 1.6 Hz, Ar-H), 7.98 (1H, d, J = 15.6 Hz, Ar-H), 8.13 (2H, t, J = 7.2 Hz, Ar-H), 8.39 (1H, d, J = 0.8 Hz, Ar-H), 8.57 (1H, s, Ar-H); ^{13}C NMR ($CDCl_3$): δ (ppm) 186.30(C=O of chalcone), 158.94(C=O of coumarin), 147.79(CH), 147.09(CH), 147.07(C), 144.90(C), 141.76(C), 140.49(C), 126.90(CH), 126.33(CH), 126.04(C), 125.98(C), 124.71(CH), 123.49(C), 122.95(C), 122.50(CH), 121.13(CH), 120.91(CH), 120.77(CH), 119.82(CH), 119.36(C), 115.56(CH),

108.90(CH), 56.40(–OCH_3 of coumarin), 37.82(CH_2 of carbazole), 13.85(CH_3 of carbazole). Anal. calcd for $C_{27}H_{21}NO_4$: elemental analysis: C, 76.58; H, 5.00; N, 3.31%. Found: C, 76.58; H, 4.98; N, 3.31%.

*4.1.1.4. (E)-2-(3-(9-Ethyl-9H-carbazol-3-yl)acryloyl)-3H-benzo [f]chromen-3-one (**3c**).* Yield: 87%; mp 240–243 °C (lit[42]); orange solid; IR spectrum, ν_{max}, cm^{-1}: 3052 (aromatic C–H stretching), 2970, 2929, 2890 (aliphatic C–H stretching), 1723 (C=O stretching of δ-lactone of coumarin), 1654 (C=O stretching of chalcone), 1572 & 1468 (C=C); ^{1}H NMR ($CDCl_3$) δ, ppm (J, Hz): 1.45 (3H, t, J = 7.2 Hz, CH_3 of carbazole), 4.36 (2H, q, J = 7.2 Hz, CH_2 of carbazole), 7.28 (1H, t, J = 7.2 Hz, Ar-H), 7.40–7.43 (2H, m, Ar-H), 7.48–7.51 (2H, m, Ar-H), 7.60 (1H, t, J = 7.2 Hz, Ar-H), 7.74 (1H, ddd, J = 8.0 Hz, 6.4 Hz, 1.2 Hz, Ar-H), 7.86 (1H, dd, J = 7.2 Hz and 1.6 Hz, Ar-H), 7.91 (1H, d, J = 8.0 Hz, Ar-H), 8.07 (1H, d, J = 9.2 Hz, Ar-H), 8.14 (3H, m, Ar-H), 8.40 (2H, d, J = 8.0 Hz, Ar-H), 9.40 (1H, s, Ar-H); ^{13}C NMR ($CDCl_3$): δ (ppm) 186.13 (C=O of chalcone), 159.66(C=O of coumarin), 155.88(C), 146.94(CH), 143.57(CH), 141.72(C), 140.47(C), 135.78(CH), 130.27(C), 129.84(C), 129.17(CH), 129.07(CH), 126.90(CH), 126.54(CH), 126.32(CH), 126.10(C), 123.86(C), 123.49(C), 122.95(C), 122.46(CH), 121.90(CH), 120.97(CH), 120.77(CH), 119.81(CH), 116.56(CH), 113.26(C), 108.89(CH), 37.80(CH_2 of carbazole), 13.85(CH_3 of carbazole). Anal. calcd for $C_{30}H_{21}NO_3$: elemental analysis: C, 81.25; H, 4.77; N, 3.16%. Found: C, 81.22; H, 4.76; N, 3.15%.

*One carbon appears equivalent in **3a**, **3b**, and **3c** compounds.

*4.1.1.5. General synthetic procedure for compounds **4a–c**, **5a–c**, **6a–c**, **7a–c**.* A mixture of various chalcone (**3a–c**) (3 mmol), various hydrazines such as semicarbazide, phenylhydrazine, 4-methyl phenylhydrazine and 3-chloro phenylhydrazine (3 mmol), and acetic acid (0.3 mmol) in 30 mL of ethanol was stirred at 65 °C for 90–180 min. It was then poured in water (75 mL), and the crude solid obtained was extracted with chloroform (3 × 50 mL). The organic layer was washed with 10% sodium bicarbonate solution (50 mL), water (50 mL), and dried over anhydrous sodium sulfate. Distillation of chloroform in vacuum gave gummy material subjected to column chromatography using petroleum ether (60–80 °C) : $CHCl_3$ (5 : 5) as an eluent to afford final products **4a–c**, **5a–c**, **6a–c**, **7a–c**.

*4.1.1.6. 5-(9-Ethyl-9H-carbazol-3-yl)-3-(2-oxo-2H-chromen-3-yl)-4,5-dihydro-1H-pyrazole-1-carboxamide (**4a**).* Yield: 71%; mp 152–154 °C; yellow solid; IR spectrum, ν_{max}, cm^{-1}: 3448 & 3277 (amine stretching), 3048 (aromatic C–H stretching), 2973, 2929 (aliphatic C–H stretching), 1730 (C=O stretching of δ-lactone of coumarin), 1666 (C=O stretching of amide), 1605 (C=N), 1572 & 1467 (C=C), 1231 & 1133 (C–N); ^{1}H NMR ($CDCl_3$) δ, ppm (J, Hz): 1.39 (3H, t, J = 7.2 Hz, –CH_3 of carbazole), 3.50 (1H, dd, J = 13.6 Hz and 5.2 Hz, Ha of pyrazoline), 4.05 (1H, dd, J = 12.0 and 6.4 Hz, Hb of pyrazoline), 4.33 (2H, q, J = 7.2 Hz, –CH_2 of carbazole), 5.40 (2H, broad singlet, –NH_2 of pyrazoline ring), 5.72 (1H, dd, J = 8.0 Hz and 5.4 Hz, Hx of pyrazoline), 7.18 (1H, t, J = 7.2 Hz, Ar-H), 7.25–7.38 (5H, m, Ar-H), 7.43 (1H, td, J = 7.6 Hz and 1.2 Hz, Ar-H), 7.54–7.59 (2H, m, Ar-H), 7.96 (1H, s, Ar-H), 8.05 (1H, d, J = 7.6 Hz, Ar-H), 8.32 (1H, s, Ar-H); ^{13}C NMR ($CDCl_3$): δ (ppm) 158.85(C=O of coumarin), 155.18(C=O of amide), 153.89(C), 148.30(C), 140.50(CH), 140.27(C), 139.45(C), 132.93(C), 132.56(CH), 128.63(CH), 125.70(CH), 124.82(CH), 123.33(CH), 121.12(C), 122.78(C), 120.55(CH), 119.70(C), 118.85(C), 118.73(CH), 117.49(CH), 116.52(CH), 108.81(CH), 108.43(CH), 61.03(CHx of pyrazoline), 45.21(CH_2 of pyrazoline), 37.52(CH_2 of carbazole), 13.79(CH_3 of carbazole). Anal. calcd for $C_{27}H_{22}N_4O_3$: elemental analysis: C, 71.99; H, 4.92; N, 12.44%. Found: C, 71.97; H, 4.93; N, 12.47%. MS m/z: 473.2 (M + 23), LCMS: 451.3 (M + 1).

*4.1.1.7. 5-(9-Ethyl-9H-carbazol-3-yl)-3-(8-methoxy-2-oxo-2H-chromen-3-yl)-4,5-dihydro-1H-pyrazole-1-carboxamide (**4b**).* Yield: 75%; mp 169–172 °C; light yellow solid; IR spectrum, ν_{max},-cm^{-1}: 3490 & 3379 (amine stretching), 3051 (aromatic C–H stretching), 2971 & 2931 (aliphatic C–H stretching), 1709 (C=O stretching of δ-lactone of coumarin), 1687 (C=O stretching of amide), 1603 (C=N), 1576 & 1480 (C=C), 1135 & 1230 (C–N); 1H NMR (DMSO-d_6) δ, ppm: 1.35 (3H, t, J = 7.2 Hz, CH_3 of carbazole), 3.38 (1H, d, J = 6.0 Hz, Ha protons of pyrazoline), 3.94 (3H, s, –OCH_3 of coumarin), 4.02 (1H, d, J = 9.6 Hz, Hb protons of pyrazoline), 4.40 (2H, q, J = 6.8 Hz, CH_2 of carbazole) 5.61 (1H, dd, J = 8.0 Hz and 5.6 Hz, Hx protons of pyrazoline), 6.46 (2H, broad singlet, –NH_2 of pyrazoline ring), 7.16 (1H, t, J = 7.2 Hz, Ar-H), 7.25 (2H, d, J = 6.0 Hz, Ar-H), 7.27–7.51 (3H, m, Ar-H), 7.94 (1H, s, Ar-H), 8.06 (1H, d, J = 7.6 Hz, Ar-H), 8.16 (2H, s, Ar-H), 8.65 (1H, s, Ar-H); ^{13}C NMR (DMSO-d_6): δ (ppm) 157.93(C=O of coumarin), 154.75(C=O of amide), 146.67(C), 146.30(C), 142.71(C), 140.88(CH), 139.74(C), 138.71(C), 133.88(C), 125.51(CH), 124.59(CH), 123.29(CH), 122.08(C), 122.00(C), 120.05(CH), 119.92(CH), 119.56(C), 119.36(C), 118.49(CH), 117.12(CH), 114.41(CH), 108.81(CH), 108.68(CH), 60.37(CHx of pyrazoline), 55.92(–OCH_3 of coumarin), 44.71(CH_2 of pyrazoline), 36.98(CH_2 of carbazole), 13.84(CH_3 of carbazole). Anal. calcd For $C_{28}H_{24}N_4O_4$: elemental analysis: C, 69.99; H, 5.03; N, 11.66%. Found: C, 69.94; H, 5.01; N, 11.69%. MS m/z: 503.2 (M + 23).

*4.1.1.8. 5-(9-Ethyl-9H-carbazol-3-yl)-3-(3-oxo-3H-benzo[f]chromen-2-yl)-4,5-dihydro-1H-pyrazole-1-carboxamide (**4c**).* Yield: 74%; mp 241–244 °C; dark yellow solid; IR spectrum, ν_{max},-cm^{-1}: 3483 & 3275 (amine stretching), 3050 (aromatic C–H stretching), 2972 & 2929 (aliphatic C–H stretching), 1726 (C=O stretching of δ-lactone of coumarin), 1680 (C=O stretching of amide), 1628 (C=N), 1567 & 1451 (C=C), 1231& 1130 (C–N); ^{1}H NMR (DMSO-d6) δ, ppm (J, Hz): 1.34 (3H, t, J = 7.2 Hz, CH_3 of carbazole), 3.46 (1H, dd, J = 16.8 Hz and 5.6 Hz Ha protons of pyrazoline), 4.02 (1H, dd, J = 12.4 Hz and 6.0 Hz, Hb protons of pyrazoline), 4.40 (2H, q, J = 7.2 Hz, –CH_2 of carbazole), 5.64 (1H, dd, J = 12.0 Hz and 5.6 Hz, Hx protons of pyrazoline), 6.72 (2H, broad singlet, –NH_2 of pyrazoline ring), 7.16 (1H, t, J = 7.6 Hz, Ar-H), 7.34–7.50 (4H, m, Ar-H), 7.51–7.64 (2H, m, Ar-H), 7.78–8.07 (5H, m, Ar-H), 8.75 (1H, d, J = 8.2 Hz, Ar-H), 9.49 (1H, s, Ar-H); ^{13}C NMR (DMSO-d6): δ (ppm) 158.46(C=O of coumarin), 154.93(C=O of amide), 153.33(C), 146.64(C), 139.74(C), 138.71(C), 136.19(CH), 134.10(C), 133.69(CH), 129.96(C), 128.99(C), 128.76(CH), 128.19(CH), 126.08(CH), 125.51(CH), 123.36(CH), 122.53(CH), 122.08(C), 122.02(C), 120.06(CH), 118.49(CH), 118.40(C), 117.17(CH), 116.20(CH), 113.26(C), 108.82(CH), 108.69(CH), 60.54(CHx of pyrazoline), 44.85(CH_2 of

pyrazoline), 36.98(CH_2 of carbazole), 13.56(CH_3 of carbazole). Anal. calcd for $C_{31}H_{24}N_4O_3$: elemental analysis: C, 74.39; H, 4.83; N, 11.19%. Found: C, 74.42; H, 4.81; N, 11.20%. MS *m*/*z*: 523.2 (M + 23).

*4.1.1.9. 3-(5-(9-Ethyl-9H-carbazol-3-yl)-1-phenyl-4,5-dihydro-1H-pyrazol-3-yl)-2H-chromen-2-one (**5a**).* Yield: 65%; mp 232–235 °C; orange solid; IR spectrum, ν_{max}, cm^{-1}: 3043 (aromatic C–H stretching), 2977 & 2930 (aliphatic C–H stretching), 1729 (C=O stretching of δ-lactone of coumarin), 1598 (C=N), 1563, 1528 & 1494 (C=C), 1231 & 1133 (C–N); ^{1}H NMR ($CDCl_3$) δ, ppm (*J*, Hz): 1.41 (3H, t, $J = 7.2$ Hz, CH_3 of carbazole), 3.47 (1H, dd, $J = 12.4$ Hz and 7.6 Hz, Ha protons of pyrazoline), 4.18 (1H, dd, $J = 12.8$ and 5.6 Hz, Hb protons of pyrazoline), 4.34 (2H, q, $J = 7.2$ Hz, CH_2 of carbazole), 5.52 (1H, dd, $J = 7.2$ Hz and 5.2 Hz, Hx protons of pyrazoline), 6.78–6.80 (1H, m, Ar-H), 7.16–7.43 (10H, m, Ar-H), 7.46 (1H, dd, $J = 8.0$ Hz and 1.2 Hz, Ar-H), 7.50 (1H, td, $J = 8.0$ Hz and 1.2 Hz, Ar-H), 7.59 (1H, dd, $J = 7.6$ Hz and 1.2 Hz, Ar-H), 8.01 (1H, s, Ar-H), 8.06 (1H, d, $J = 7.6$ Hz, Ar-H), 8.43 (1H, s, Ar-H); ^{13}C NMR ($CDCl_3$): δ (ppm) 159.68(C=O of coumarin), 153.56(C), 144.34(C), 143.05(C), 140.32(C), 139.47(C), 137.48(CH), 132.80(C), 131.40(CH), 128.95(CH), 128.16(CH), 127.70(CH), 126.57(CH), 126.11(CH), 125.55(CH), 124.68(CH), 123.35(C), 121.06(CH), 120.55(CH), 119.76(C), 119.59(CH), 118.86(C), 117.73(C), 116.42(CH), 113.82(C), 109.16(CH), 108.53(CH), 108.37(CH), 65.60(CHx of pyrazoline), 45.86(CH_2 of pyrazoline), 37.62(CH_2 of carbazole), 13.84(CH_3 of carbazole). Anal. calcd for $C_{32}H_{25}N_3O_2$: elemental analysis: C, 79.48; H, 5.21; N, 8.69%. Found: C, 79.51; H, 5.22; N, 8.68%. MS *m*/*z*: 506.2 (M + 23).

*4.1.1.10. 3-(5-(9-Ethyl-9H-carbazol-3-yl)-1-phenyl-4,5-dihydro-1H-pyrazol-3-yl)-8-methoxy-2H-chromen-2-one (**5b**).* Yield: 64%; mp 136–138 °C; dark-orange solid; IR spectrum, ν_{max}, cm^{-1}: 3046 (aromatic C–H stretching), 2971 & 2931 (aliphatic C–H stretching), 1727 (C=O stretching of δ-lactone of coumarin), 1598 (C=N), 1571 & 1495 (C=C), 1131 & 1231 (C–N); ^{1}H NMR ($CDCl_3$) δ, ppm (*J*, Hz): 1.41 (3H, t, $J = 7.2$ Hz, CH_3 of carbazole), 3.46 (1H, dd, $J = 14.8$ Hz and 7.6 Hz, Ha protons of pyrazoline), 3.95 (3H, s, –OCH_3), 4.18 (1H, dd, $J = 12.4$ and 6.0 Hz Hb protons of pyrazoline), 4.33 (2H, q, $J = 7.2$ Hz, CH_2 of carbazole), 5.51 (1H, dd, $J = 7.6$ Hz and 4.8 Hz, Hx protons of pyrazoline), 6.79 (1H, t, $J = 2.8$ Hz, Ar-H), 7.03–7.46 (12H, m, Ar-H), 8.00 (1H, s, Ar-H), 8.05 (1H, d, $J = 8.4$ Hz, Ar-H), 8.41 (1H, s, Ar-H); ^{13}C NMR (DMSO-d_6): δ (ppm) 159.14(C=O of coumarin), 146.98(C), 144.37(C), 143.14(C), 140.33(CH), 139.47(C), 137.66(CH), 132.81(C), 129.04(CH), 128.95(CH), 127.69(C), 125.84(CH), 125.56(CH), 124.50(CH), 124.35(C), 123.43(CH), 122.65(C), 121.28(C), 120.56(CH), 120.24(C), 119.75(CH), 119.71(C), 118.85(CH), 117.74(CH), 113.83(CH), 113.41(CH), 109.15(CH), 108.53(CH), 65.64(CHx of pyrazoline), 56.28(–OCH_3), 45.89(CH_2 of pyrazoline), 37.69(CH_2 of carbazole), 13.84(CH_3 of carbazole). Anal. calcd for chemical formula: $C_{33}H_{27}N_3O_3$: elemental analysis: C, 77.17; H, 5.30; N, 8.18%. Found: C, 77.20; H, 5.27; N, 8.16%. MS *m*/*z*: 536.2 (M + 23).

*4.1.1.11. 2-(5-(9-Ethyl-9H-carbazol-3-yl)-1-phenyl-4,5-dihydro-1H-pyrazol-3-yl)-3H-benzo[f] chromen-3-one (**5c**).* Yield: 68%; mp 243–245 °C; Crimson-red solid; IR spectrum, ν_{max}, cm^{-1}: 3051 (aromatic C–H stretching), 2978 & 2930 (aliphatic C–H stretching), 1726 (C=O stretching of δ-lactone of coumarin), 1595 (C=N), 1561 & 1467 (C=C), 1136 & 1228 (C–N); ^{1}H NMR (DMSO-d_6) δ, ppm (*J*, Hz): 1.29 (3H, t, $J = 7.2$ Hz, CH_3 of carbazole), 3.44 (1H, d, $J = 6.0$ Hz, Ha protons of pyrazoline), 4.14 (1H, dd, $J = 12.8$ Hz and 5.2 Hz, Hb protons of pyrazoline), 4.41 (2H, q, $J = 7.2$ Hz, CH_2 of carbazole), 5.72 (1H, dd, $J = 6.4$ Hz and 6.0 Hz, Hx protons of pyrazoline), 6.74 (1H, t, $J = 6.8$ Hz, Ar-H), 7.15–7.67 (11H, m, Ar-H), 7.75 (1H, t, $J = 7.6$ Hz, Ar-H) 8.07 (1H, dd, $J = 7.2$ Hz, Ar-H), 7.13 (2H, t, $J = 7.6$ Hz, Ar-H), 8.19 (1H, d, $J = 9.2$ Hz, Ar-H), 9.10 (1H, s, Ar-H); ^{13}C NMR ($CDCl_3$): δ (ppm) 159.83(C=O of coumarin), 153.32(C), 144.31(C), 143.43(C), 140.30(C), 139.46(C), 133.22(CH), 132.83(CH), 130.46(C), 129.19(C), 129.06(CH), 129.01(CH), 128.29(CH), 126.21(CH), 125.86(CH), 123.42(CH), 123.33(C), 122.62(C), 121.95(CH), 120.58(CH), 119.84(C), 119.78(CH), 118.86(CH), 117.75(CH), 116.63(CH), 113.92(C), 113.82(CH), 109.19(CH), 108.54(CH), 65.61(CHx of pyrazoline), 45.92(CH_2 of pyrazoline), 37.62(CH_2 of carbazole), 13.88(CH_3 of carbazole). Anal. calcd for $C_{36}H_{27}N_3O_2$: elemental analysis: C, 81.03; H, 5.10; N, 7.87%. Found: C, 81.06; H, 5.12; N, 7.89%. MS *m*/*z*: 556.2 (M + 23).

*4.1.1.12. 3-(5-(9-Ethyl-9H-carbazol-3-yl)-1-(p-tolyl)-4,5-dihydro-1H-pyrazol-3-yl)-2H-chromen-2-one (**6a**).* Yield: 66%; mp 221–223 °C; orange solid; IR spectrum, ν_{max}, cm^{-1}: 3033 (aromatic C–H stretching), 2975 & 2915 (aliphatic C–H stretching) 1725 (C=O stretching of δ-lactone of coumarin), 1604 (C=N), 1562 & 1465 (C=C), 1134 & 1230 (C–N); ^{1}H NMR ($CDCl_3$) δ, ppm (*J*, Hz): 1.44 (3H, t, $J = 7.2$ Hz, CH_3 of carbazole), 2.24 (3H, s, –CH_3), 3.48 (1H, dd, $J = 10.4$ Hz and $J = 8.0$ Hz, Ha protons of pyrazoline), 4.19 (1H, dd, $J = 12.8$ and 5.2 Hz, Hb protons of pyrazoline), 4.36 (2H, q, $J = 7.2$ Hz, CH_2 of carbazole), 5.51 (1H, dd, $J = 8.0$ Hz and 4.8 Hz, Hx protons of pyrazoline), 7.0 (2H, d, $J = 8.4$ Hz, Ar-H), 7.10 (2H, d, $J = 8.4$ Hz, Ar-H), 7.23 (1H, t, $J = 7.2$ Hz, Ar-H), 7.28–7.39 (2H, m, Ar-H), 7.46–7.54 (2H, m, Ar-H), 7.40 (3H, t, $J = 6.8$, Ar-H), 7.60 (1H, d, $J = 7.6$ Hz, Ar-H), 8.04 (1H, s, Ar-H), 8.08 (1H, d, $J = 7.6$ Hz, Ar-H), 8.43 (1H, s, Ar-H); ^{13}C NMR-APT ($CDCl_3$): δ (ppm) 159.74(C=O of coumarin), 153.46(C), 142.48(C), 142.14(C), 140.28(C), 139.42(C), 137.15(CH), 132.89(C), 131.29(CH), 129.50(CH), 129.09(C), 128.11(CH), 125.82(CH), 124.67(CH), 123.46(CH), 123.29(C), 122.63(C), 121.10(C), 120.57(CH), 119.63(C), 118.83(CH), 117.79(CH), 116.40(CH), 113.87(CH), 109.13(CH), 108.52(CH), 65.83(CHx of pyrazoline), 45.80(CH_2 of pyrazoline), 37.61(CH_2 of carbazole), 20.55(CH_3 of pendant phenyl ring), 13.84(CH_3 of carbazole). Anal. calcd for $C_{33}H_{27}N_3O_2$: elemental analysis: C, 79.66; H, 5.47; N, 8.44%. Found: C, 79.72; H, 5.50; N, 8.42%. MS *m*/*z*: 520.1 (M + 23).

*4.1.1.13. 3-(5-(9-Ethyl-9H-carbazol-3-yl)-1-(p-tolyl)-4,5-dihydro-1H-pyrazol-3-yl)-8-methoxy-2H-chromen-2-one (**6b**).* Yield: 56%; mp 124–126 °C; red solid; IR spectrum, ν_{max}, cm^{-1}: 3040 (aromatic C–H stretching), 2971 & 2930 (aliphatic C–H stretching) 1726 (C=O stretching of δ-lactone of coumarin), 1606 (C=N), 1572 & 1479 (C=C), 1232 (C–N); ^{1}H NMR ($CDCl_3$) δ, ppm (*J*, Hz): δ (ppm) 1.43 (3H, t, $J = 7.2$ Hz, CH_3 of carbazole), 2.24 (3H, s, –CH_3), 3.47 (1H, dd, $J = 10.4$ Hz and 8.0 Hz, Ha protons of pyrazoline), 3.98 (3H, s, –OCH_3), 4.20 (1H, dd, $J = 12.4$ Hz and 5.6 Hz, Hb protons of pyrazoline), 4.36 (2H, q, $J = 7.2$ Hz, –CH_2 of carbazole), 5.50 (1H, dd, $J = 8.0$ Hz and 4.8 Hz, Hx protons of

pyrazoline), 6.99 (2H, d, J = 8.4 Hz, Ar-H), 7.05–7.52 (10H, m, Ar-H), 8.03 (1H, s, Ar-H), 8.08 (1H, d, J = 7.6 Hz, Ar-H), 8.41 (1H, s, Ar-H); ^{13}C NMR ($CDCl_3$): δ (ppm) 159.14(C=O of coumarin), 146.98(C), 144.37(C), 143.14(C), 140.33(C), 139.47(C), 137.66(CH), 132.81(C), 129.04(CH), 128.95(CH), 127.69(C), 125.84(CH), 125.56(CH), 124.50(CH), 124.35(C), 123.43(CH), 122.65(C), 121.28(C), 120.56(CH), 120.24(C), 119.75(CH), 119.71(C), 118.85(CH), 117.74(CH), 113.83(CH), 113.41(CH), 109.15(CH), 108.53(CH), 65.64(CHx of pyrazoline), 56.28(–OCH_3 of coumarin ring), 45.89(CH_2 of pyrazoline), 37.69(CH_2 of carbazole), 20.55(CH_3 of Pendant phenyl ring), 13.84(CH_3 of carbazole). Anal. calcd for $C_{34}H_{29}N_3O_3$: elemental analysis: C, 77.40; H, 5.54; N, 7.96%. Found: C, 77.38; H, 5.47; N, 7.96%. MS m/z: 550.2 (M + 23).

*4.1.1.14. 2-(5-(9-Ethyl-9H-carbazol-3-yl)-1-(p-tolyl)-4,5-dihydro-1H-pyrazol-3-yl)-3H-benzo[f] chromen-3-one (**6c**).* Yield: 65%; mp 229–232 °C; Crimson red solid; IR spectrum, ν_{max}, cm^{-1}: 3049 (aromatic C–H stretching), 2977 & 2910 (aliphatic C–H stretching) 1727 (C=O stretching of δ-lactone of coumarin), 1608 (C=N) 1560 & 1466 (C=C), 1227 & 1136 (C–N); ^{1}H NMR ($CDCl_3$) δ, ppm (J, Hz): 1.44 (3H, t, J = 7.2 Hz, CH_3 of carbazole), 2.26 (3H, s, –CH_3), 3.54 (1H, dd, J = 10.8 Hz and 7.6 Hz, Ha protons of pyrazoline), 4.25 (1H, dd, J = 8.8 and 5.6 Hz, Hb protons of pyrazoline), 4.36 (2H, q, J = 7.2 Hz, –CH_2 of carbazole), 5.54 (1H, dd, J = 7.6 Hz and 4.8 Hz, Hx protons of pyrazoline), 7.03 (2H, d, J = 8.4 Hz, Ar-H), 7.16 (2H, d, J = 8.4 Hz, Ar-H), 7.22 (1H, d, J = 7.6 Hz, Ar-H), 7.37–7.49 (5H, m, Ar-H), 7.61 (1H, t, J = 8.0 Hz, Ar-H), 7.76 (1H, t, J = 7.6 Hz, Ar-H), 7.94 (2H, t, J = 9.6 Hz, Ar-H), 8.07–8.10 (2H, m, Ar-H), 8.46 (1H, d, J = 8.4 Hz, Ar-H), 9.21 (1H, s, Ar-H); ^{13}C NMR ($CDCl_3$): δ (ppm) 159.85(C=O of coumarin), 153.20(C), 142.89(C), 142.18(C), 140.28(C), 139.43(C), 132.95(C), 132.84(CH), 132.65(CH), 130.45(C), 129.53(CH), 129.17(C), 129.11(C), 129.03(CH), 128.23(CH), 126.16(CH), 125.82(CH), 123.48(CH), 123.31(C), 122.64(C), 121.96(CH), 120.58(CH), 119.93(C), 119.27(C), 118.83(CH), 117.80(CH), 116.62(CH), 113.92(CH), 109.14(CH), 108.52(CH), 65.89(CHx of pyrazoline), 45.86(CH_2 of pyrazoline), 37.61(CH_2 of carbazole), 20.59(CH_3 of Pendant phenyl ring), 13.87(CH_3 of carbazole). Anal. calcd for $C_{37}H_{29}N_3O_2$: elemental analysis: C, 81.15; H, 5.34; N, 7.67%. Found: C, 81.18; H, 5.31; N, 7.66%. MS m/z: 570.2 (M + 23).

*4.1.1.15. 3-(1-(3-Chlorophenyl)-5-(9-ethyl-9H-carbazol-3-yl)-4,5-dihydro-1H-pyrazol-3-yl)-2H-chromen-2-one (**7a**).* Yield: 70%; mp 189–191 °C; light orange solid; IR spectrum, ν_{max}, cm^{-1}: 3046 (aromatic C–H stretching), 2975 & 2929 (aliphatic C–H stretching), 1727 (C=O stretching of δ-lactone of coumarin), 1594 (C=N), 1562 & 1481 (C=C); ^{1}H NMR ($CDCl_3$) δ, ppm (J, Hz): 1.46 (3H, t, J = 7.2 Hz, CH_3 of carbazole), 3.54 (1H, dd, J = 11.2 Hz and 7.6 Hz, Ha protons of pyrazoline), 4.22 (1H, dd, J = 12.4 Hz and 6.0 Hz, Hb protons of pyrazoline), 4.38 (2H, q, J = 7.6 Hz, CH_2 of carbazole), 5.53 (1H, dd, J = 7.6 Hz and 5.4 Hz, Hx protons of pyrazoline), 6.79 (1H, d, J = 7.6 Hz, Ar-H), 6.89 (1H, d, J = 7.6 Hz and 1.2 Hz, Ar-H), 7.06 (1H, t, J = 8.0 Hz, Ar-H), 7.25 (1H, d, J = 7.6 Hz, Ar-H), 7.30–7.57 (8H, m, Ar-H), 7.65 (1H, d, J = 7.6 Hz, Ar-H), 8.02 (1H, s, Ar-H), 8.11 (1H, d, J = 7.6 Hz, Ar-H), 8.50 (1H, s, Ar-H); ^{13}C NMR ($CDCl_3$): δ (ppm) 159.64(C=O of coumarin), 153.66(C), 145.26(C), 144.14(C), 140.34(C), 139.55(C), 138.20(CH), 134.82(C), 132.18(C), 131.73(CH), 129.98(CH), 128.37(CH), 125.98(CH), 124.80(CH), 123.42(C), 123.27(CH), 122.58(C), 120.68(C), 120.60(C), 120.59(CH), 119.47(CH), 118.96(CH), 117.64(CH), 116.47(CH), 113.94(CH), 111.54(CH), 109.29(CH), 108.62(CH), 65.28(CHx of pyrazoline), 46.04(CH_2 of pyrazoline), 37.66(CH_2 of carbazole), 13.89(CH_3 of carbazole). Anal. calcd for $C_{32}H_{24}ClN_3O_2$: elemental analysis: C, 74.20; H, 4.67; N, 8.11%. Found: C, 74.19; H, 4.70; N, 8.13%. MS m/z: 540.2 (M + 23).

*4.1.1.16. 3-(1-(3-Chlorophenyl)-5-(9-ethyl-9H-carbazol-3-yl)-4,5-dihydro-1H-pyrazol-3-yl)-8-methoxy-2H-chromen-2-one (**7b**).* Yield: 68%; mp 130–132 °C; orange solid; IR spectrum, ν_{max}, cm^{-1}: 3049 & 2930 (aromatic C–H), 1727 (C=O, δ-lactone), 1592 (C=N), 1484 (C=C), 1274 & 1271(C–N); ^{1}H NMR ($CDCl_3$) δ, ppm (J, Hz): 1.48 (3H, t, J = 7.6 Hz, –CH_3 of carbazole), 3.51 (1H, dd, J = 11.6 Hz and 7.6 Hz, Ha protons of pyrazoline), 3.98 (3H, t, J = 11.2 Hz, –OCH_3), 4.22 (1H, dd, J = 12.4 Hz and 6.0 Hz, Hb protons of pyrazoline), 4.35 (2H, m, CH_2 of carbazole), 5.50 (1H, dd, J = 7.2 Hz and 5.6 Hz, Hx protons of pyrazoline), 6.75 (1H, d, J = 8.0 Hz, Ar-H), 6.85 (1H, d, J = 8.0 Hz, Ar-H), 7.05 (1H, t, J = 8.0 Hz, Ar-H), 7.09 (1H, d, J = 8.0 Hz, Ar-H), 7.20–7.24 (3H, m, Ar-H), 7.36–7.40 (3H, m, Ar-H), 7.41 (1H, d, J = 8.4 Hz, Ar-H), 7.46 (1H, d, J = 7.2 Hz, Ar-H), 7.99 (1H, s, Ar-H), 8.08 (1H, d, J = 8.8 Hz, Ar-H), 8.48 (1H, s, Ar-H); ^{13}C NMR (CDCl3): δ (ppm) 159.08(C), 146.93(C), 145.24(C), 144.19(C), 143.24(C), 140.30(C), 139.51(C), 138.37(CH), 134.77(C), 132.14(C), 129.94(CH), 125.92(CH), 124.61(CH), 123.36(C), 123.25(CH), 122.55(C), 120.86(C), 120.57(CH), 120.07(C), 119.80(CH), 119.41(CH), 118.90(CH), 117.59(CH), 113.89(CH), 113.54(CH), 111.48(CH), 109.24(CH), 108.57(CH), 65.28(CHx of pyrazoline), 56.24(–OCH_3 of coumarin), 46.03(CH_2 of pyrazoline), 37.62(CH_2 of carbazole), 13.87(CH_3 of carbazole). Anal. calcd for $C_{33}H_{26}ClN_3O_3$: elemental analysis: C, 72.32; H, 4.78; N, 7.67%. Found: C, 72.18; H, 4.81; N, 7.65%. MS m/z: 570.2 (M + 23).

*4.1.1.17. 2-(1-(3-Chlorophenyl)-5-(9-ethyl-9H-carbazol-3-yl)-4,5-dihydro-1H-pyrazol-3-yl)-3H-benzo[f]chromen-3-one (**7c**).* Yield: 61%; mp 234–236 °C; orange solid; IR spectrum, ν_{max}, cm^{-1}: 3051 (aromatic C–H stretching), 2976 & 2930 (aliphatic C–H stretching) 1727 (C=O stretching of δ-lactone of coumarin), 1592 (C=N), 1561 & 1483 (C=C), 1132 & 1228 (C–N); ^{1}H NMR ($CDCl_3$) δ, ppm (J, Hz): 1.44 (3H, s, CH_3 of carbazole), 3.57 (1H, d, J = 13.2 Hz, Ha protons of pyrazoline), 4.31 (3H, m, Hb proton of pyrazoline and CH_2 of carbazole), 5.55 (1H, s, Hx proton of pyrazoline), 6.80 (1H, s, Ar-H), 6.94 (1H, s, Ar-H), 7.07 (1H, s, Ar-H), 7.23 (1H, s, Ar-H), 7.40–7.47 (6H, m, Ar-H), 7.63 (1H, s, Ar-H), 7.79 (1H, s, Ar-H), 7.93–8.10 (4H, m, Ar-H), 8.49 (1H, d, J = 6.8 Hz, Ar-H), 9.25 (1H, s, Ar-H); ^{13}C NMR ($CDCl_3$): δ (ppm) 159.75(C=O of coumarin), 153.51(C), 145.22(C), 144.55(C), 140.31(C), 139.52(C), 134.81(C), 133.85(CH), 133.17(CH), 132.20(C), 130.49(C), 130.45(C), 129.98(CH), 129.19(C), 129.07(CH), 128.43(CH), 126.30(CH), 125.94(CH), 123.40(C), 123.25(CH), 122.56(C), 122.00(CH), 120.58(CH), 119.46(CH), 118.92(CH), 117.61(CH), 116.60(CH), 113.89(CH), 113.82(C), 111.58(CH), 109.27(CH), 108.58(CH), 65.28(CHx of pyrazoline), 46.06(CH_2 of pyrazoline), 37.64(CH_2 of carbazole), 13.88(CH_3 of carbazole). Anal. calcd for $C_{36}H_{26}ClN_3O_2$:

elemental analysis: C, 76.12; H, 4.61; N, 7.40%. Found: C, 76.19; H, 4.60; N, 7.42%. MS *m*/*z*: 590.2 (M + 23).

*4.1.1.18. General synthetic procedure for compounds **8a–c**.* A mixture of various coumarin–carbazole chalcone (**3a–c**) (3 mmol), hydrazine hydrate (6 mmol), and acetic acid (6 mmol) in 30 mL of ethanol was stirred at 65 °C for 90–180 min. It was then poured in water (75 mL), and the crude solid obtained was extracted with chloroform (3 × 50 mL). The organic layer was washed with 10% sodium bicarbonate solution (50 mL), water (50 mL), and dried over anhydrous sodium sulfate. Distillation of chloroform in vacuum gave gummy material subjected to column chromatography using petroleum ether (60–80 °C) : $CHCl_3$ (5 : 5) as an eluent to afford product **8a–c**.

*4.1.1.19. 3-(1-Acetyl-5-(9-ethyl-9H-carbazol-3-yl)-4,5-dihydro-1H-pyrazol-3-yl)-2H-chromen-2-one (**8a**).* Yield: 70%; mp 200–202 °C; greenish yellow solid; IR spectrum, ν_{max}, cm^{-1}: 3049 (aromatic C–H stretching), 2976 & 2930 (aliphatic C–H stretching) 1722 (C=O stretching of δ-lactone of coumarin), 1659 (C=O stretching of acetyl), 1606 (C=N), 1568&1486 (C=C), 1231 & 1146 (C–N); ^{1}H NMR (DMSO-d_6) δ, ppm (*J*, Hz): 1.29 (3H, t, J = 7.2 Hz, CH_3 of carbazole), 2.34 (3H, s, –CH_3 of acetyl), 3.37 (1H, m, Ha protons of pyrazoline), 3.98 (1H, dd, J = 12.0 Hz and J = 6.8 Hz, Hb protons of pyrazoline), 4.41 (2H, q, J = 7.6 Hz, –CH_2 of carbazole), 5.70 (1H, dd, J = 7.2 Hz and 4.8 Hz, Hx protons of pyrazoline), 7.17 (1H, t, J = 7.2 Hz, Ar-H), 7.30 (1H, dd, J = 6.8 Hz and 1.6 Hz, Ar-H), 7.38–7.45 (3H, m, Ar-H), 7.57 (2H, t, J = 8.0 Hz, Ar-H), 7.67 (1H, t, J = 8.0 Hz, Ar-H), 7.87 (1H, dd, J = 6.4 Hz and J = 1.2 Hz, Ar-H), 7.98 (1H, d, J = 1.2 Hz, Ar-H), 8.14 (1H, d, J = 7.6 Hz, Ar-H), 8.61 (1H, s, Ar-H); ^{13}C NMR (DMSO-d_6): δ (ppm) 167.67(C=O of acetyl), 157.94(C=O of coumarin), 153.43(C), 150.76(C), 141.78(CH), 139.81(C), 138.78(C), 132.92(CH), 129.31(CH), 126.13(C), 125.77(CH), 124.87(CH), 123.49(CH), 122.01(C), 121.93(C), 120.39(CH), 119.24(C), 118.72(C), 118.63(CH), 117.48(CH), 116.02(CH), 109.25(CH), 109.08(CH), 59.81(CHx of pyrazoline), 44.31(CH_2 of pyrazoline), 36.93(CH_2 of carbazole), 21.81(CH_3 of pendant acetyl group), 13.66(CH_3 of carbazole). Anal. calcd for $C_{28}H_{23}N_3O_3$: elemental analysis: C, 74.82; H, 5.16; N, 9.35%. Found: C, 74.87; H, 5.12; N, 9.36%. MS *m*/*z*: 472.2 (M + 23).

*4.1.1.20. 3-(1-Acetyl-5-(9-ethyl-9H-carbazol-3-yl)-4,5-dihydro-1H-pyrazol-3-yl)-8-methoxy-2H-chromen-2-one (**8b**).* Yield: 68%; mp 246–247 °C; yellow solid; IR spectrum, ν_{max}, cm^{-1}: 3048 (aromatic C–H stretching), 2964 & 2928 (aliphatic C–H stretching), 1724 (C=O stretching of δ-lactone of coumarin), 1660 (C=O stretching of acetyl), 1604 (C=N), 1573 & 1482 (C=C), 1143 & 1231 (C–N); ^{1}H NMR (DMSO-d_6) δ, ppm (*J*, Hz): 1.39 (3H, t, J = 7.2 Hz, CH_3 of carbazole), 2.44 (3H, s, –CH_3 of acetyl), 3.54 (1H, dd, J = 14.4 Hz and J = 4.4 Hz, Ha protons of pyrazoline), 3.97 (3H, s, –OCH_3), 4.04 (1H, dd, J = 12.0 Hz and 7.2 Hz, Hb protons of pyrazoline), 4.31 (2H, q, J = 7.2 Hz, –CH_2 of carbazole), 5.78 (1H, dd, J = 7.6 Hz and 4.4 Hz, Hx protons of pyrazoline), 7.12 (1H, d, J = 8.0 Hz, Ar-H), 7.15–7.45 (7H, m, Ar-H), 7.93 (1H, s, Ar-H), 8.05 (1H, d, J = 7.6 Hz, Ar-H), 8.44 (1H, s, Ar-H); ^{13}C NMR (DMSO-d_6): δ (ppm) 169.05(C=O of acetyl), 158.75(C=O of coumarin), 150.93(C), 147.20(C), 143.91(C), 141.07(CH), 140.41(C), 139.58(C), 132.39(C), 125.79(CH), 124.87(CH), 123.65(CH), 123.22(C), 122.88(C), 120.66(CH), 120.28(C), 120.19(CH), 119.62(C), 118.83(CH), 117.71(CH), 114.63(CH), 108.84(CH), 108.52(CH), 60.99(CHx of pyrazoline), 56.42(–OCH_3 of coumarin), 44.89(CH_2 of pyrazoline), 37.66(CH_2 of carbazole), 22.20(CH_3 of pendant acetyl group), 13.90(CH_3 of carbazole). Anal. calcd for $C_{29}H_{25}N_3O_4$: elemental analysis: C, 72.64; H, 5.26; N, 8.76%. Found: C, 72.58; H, 5.31; N, 8.74%. MS *m*/*z*: 502.2 (M + 23).

*4.1.1.21. 2-(1-Acetyl-5-(9-ethyl-9H-carbazol-3-yl)-4,5-dihydro-1H-pyrazol-3-yl)-3H-benzo[f]chromen-3-one (**8c**).* Yield: 61%; mp 158–160 °C; dark yellow solid; IR spectrum, ν_{max}, cm^{-1}: 3051 (aromatic C–H stretching), 2974 & 2932 (aliphatic C–H stretching), 1731 (C=O stretching of δ-lactone of coumarin), 1660 (C=O stretching of acetyl), 1600 (C=N), 1568 & 1489 (C=C), 1144 & 1228 (C–N); ^{1}H NMR (DMSO-d_6) δ, ppm (*J*, Hz): 1.29 (3H, t, J = 7.2 Hz, –CH_3 of carbazole), 2.41 (3H, s, –CH_3 of acetyl), 3.50 (1H, dd, J = 13.6 Hz and 4.8 Hz, Ha protons of pyrazoline), 4.03 (1H, dd, J = 12.0 Hz and 6.4 Hz, Hb protons of pyrazoline), 4.41 (2H, q, J = 7.2 Hz, CH_2 of carbazole), 5.73 (1H, dd, J = 7.2 Hz and 4.8 Hz, Hx protons of pyrazoline), 7.17 (1H, t, J = 7.2 Hz, Ar-H), 7.34 (1H, dd, J = 6.8 Hz and J = 2.0 Hz, Ar-H), 7.43 (1H, t, J = 7.6 Hz, Ar-H), 7.58–7.62 (3H, m, Ar-H), 7.64 (1H, t, J = 7.2 Hz, Ar-H), 7.76 (1H, t, J = 8.0 Hz, Ar-H), 8.02 (1H, d, J = 1.2 Hz, Ar-H), 8.05 (1H, d, J = 7.6 Hz, Ar-H), 8.15 (1H, d, J = 7.6 Hz, Ar-H), 8.23 (1H, d, J = 9.2 Hz, Ar-H), 8.67 (1H, d, J = 8.8 Hz, Ar-H), 9.18 (1H, s, Ar-H); ^{13}C NMR (DMSO-d_6): δ (ppm) 167.82(C=O of acetyl), 157.63(C=O of coumarin), 153.49(C), 150.84(C), 139.79(C), 138.79(C), 137.60(CH), 134.35(CH), 133.04(C), 129.93(C), 128.93(CH), 128.81(C), 128.55(CH), 126.32(CH), 125.74(CH), 123.54(CH), 122.55(CH), 122.03(C), 121.95(C), 120.39(CH), 118.63(CH), 118.24(C), 117.54(CH), 116.42(CH), 112.88(C), 109.24(CH), 109.07(CH), 59.82(CHx of pyrazoline), 44.24(CH_2 of pyrazoline), 36.93(CH_2 of carbazole), 21.90(CH_3 of pendant acetyl group),13.65(CH_3 of carbazole). Anal. calcd for $C_{32}H_{25}N_3O_3$: elemental analysis: C, 76.94; H, 5.04; N, 8.41%. Found: C, 76.98; H, 5.01;; N, 8.38%. MS *m*/*z*: 522.2 (M + 23).

4.2. Cell culture

The cervical cancer cell line HeLa, lung cancer cell line NCI-H520 and normal rat kidney epithelial cell line NRK-52E were procured from the National Centre for Cell Science, Pune, India. All the cell lines were grown on 25 cm^2 vented culture flasks (Corning, USA). HeLa and NRK-52E cell lines grown using Dulbecco's Modified Eagle Medium (DMEM) (Thermofisher, USA) and NCI-H520 cell line grown using Roswell Park Memorial Institute (RPMI) (Thermofisher, USA) respectively, supplemented with 10% heat-inactivated fetal bovine serum (Thermofisher, USA), and 100 U mL^{-1} penicillin, 100 μg mL^{-1} streptomycin and 0.25 μg mL^{-1} amphotericin B (Thermofisher, USA), in a 37 °C incubator with 5% CO_2 and 95% humidity.

4.3. Cytotoxicity assay

Cytotoxicity of synthesized compounds was tested utilizing MTT [3-(4,5-dimethylthiazol-2-yl)-2,5-diphenyltetrazolium bromide] assay. The cells were briefly seeded in triplicates into a 96-wells tissue culture plate at a density of 10^4 cells per well and incubated for 24 h at 37 °C with 5% CO_2. The wells were then treated

with the compounds tested at concentrations ranging from 5 to 300 μM and incubated further at 37 °C for 24 h. After the incubation period, the compounds were aspirated, and the wells were washed with phosphate-buffered saline (PBS). Afterward, 300 μL of media and 25 μL of MTT solution (5 mg mL^{-1} in PBS) were added to each well, followed by 3 h of incubation. Later, MTT was removed, and the formed crystal formazan was dissolved in 100 μL dimethyl sulfoxide (DMSO). The MTT assay absorbance was measured at 570 nm on an ELISA plate reader (Molecular Devices, USA). The relationship between surviving cells and drug concentration was plotted to get each cell line's survival curve after treatment with the specified compound. The 50% inhibitory concentration (IC_{50}), the concentration required to cause toxic effects in 50% of intact cells, was estimated using nonlinear regression analysis using Graph pad prism (version 7.0) software.

4.4. Cell cycle analysis

The effect of compounds **4a** and **7b** on cell cycle progression was analyzed using the propidium iodide staining. Firstly, HeLa and NCI-H520 cells were seeded into the 6-well plate at the density of 1×10^5 cells and incubated for 24 h at 37 °C with 5% CO_2. The cells were then treated with the IC_{50} concentrations of compounds **4a** and **7b**. After 24 h incubation, the cells were fixed with ice-cold 70% ethanol at −20 °C for 16 h. After fixation, cells were washed with Dulbecco's Phosphate-Buffered Saline (DPBS) (GIBCO®, Thermo Scientific) and allowed to incubate in DPBS containing Triton X-100 (0.2%) at 4 °C for 45 min. The cells were then treated with RNase A (100 μg mL^{-1}) and incubated at 37 °C for 1 h. Finally, cells were stained with Propidium Iodide (20 μg mL^{-1}) for 30 min and analyzed on the Muse™ Cell Analyzer (Luminex, USA).

4.5 Apoptosis analysis

Apoptosis assay of potent compounds **4a** and **7b** was carried out using Muse annexin V & dead cell kit (MCH100105) on Muse cell analyzer. It analyzes and gives statistics about non-apoptotic cells, early apoptotic cells, late apoptotic cells, dead cells, and nuclear debris. During the investigation of the impact of compounds **4a** and **7b** on cell lines, cultured cells were treated with an appropriate concentration of compounds for appropriate incubation time to induce apoptosis. They then treated cells were trypsinized and washed with cold PBS. Next, cells were resuspended in 1% BSA and 1% FBS. After that 100 μL of the cell, the suspension was taken in a vial and mixed with 100 μL of Muse Annexin V & Dead cell reagent. The mixture was incubated for 20 minutes at room temperature and processed for apoptosis analysis on Muse Cell Analyzer.

4.6. Detection of morphological changes

HeLa and NCI-H520 cells were seeded in a 6-well cell culture plate and incubated for 24 h at 37 °C with 5% CO_2 supply. The cells were treated at IC_{50} concentrations of compound **4a** (μM) and **7b** (μM) and allowed to incubate for 24 h. After the incubation, cells were washed and fixed with 4% *p*-formaldehyde for 15 min and permeabilized with 0.1% Triton X-100. The cells were stained using DAPI (1 mg mL^{-1}) for 10 min and observed under a fluorescence microscope (brand) with the DAPI excitation filter. The images were processed and analyzed by ZEN 3.2 (blue edition).

4.7. Molecular docking studies

The structure of ligands was prepared in ChemDraw Ultra v19.0 and assigned appropriate 2D orientation. The drawn structures were analyzed for connection error in bond order. The molecules' energy minimization was carried out by Chem3D ultra using MMFF94 forcefield and 0.1 RMS gradient. Molecular docking analysis of compound **4a** and **7b** showing the highest *in vitro* cytotoxicity was performed to determine the binding mechanism of these compounds with the target protein CDK2. The target protein CDK2 (PDB ID: 2A4L) was extracted from Protein Data Bank (PDB). Initially, the PDB files of selected proteins were processed by deleting ligands and non-proteins using Discover Studio visualizer v20.1.0.19295. Further, the protein structures were prepared by removing water molecules and then the addition of Kollman charges and polar hydrogen atoms. Next, the ligands were processed by merging Gastiger charges to their structures. Finally, both ligand and protein structures were converted to pdbqt file using AutoDock Tools 1.5.6. AutodockVina v1.1.2 carried out docking calculations.[43] The dimension of the grid used for both the proteins was kept $40 \times 40 \times 40$ Å and separated by 0.375 Å grid-point spacing. The *X*, *Y*, and *Z* coordinates (grid centers) in the grid were specified, which differed for both the receptors (Table 2). The exhaustiveness for the docking run was set to the default value of eight. The ligand's binding energy was calculated using the default Lamarckian genetic algorithm of the AutoDock Vina software package. After completing the docking run, the protein–ligand complexes were analyzed using Biovia Discovery Studio Visualizer v20.1.0.19295 and Pymol molecular graphics software. Biovia Discovery Studio Visualizer v20.1.0.19295 generated the representative 2D and 3D structures showing protein–ligand structures.

4.8. Statistical analysis

The data are shown as mean ± SE of triplicate independent analysis. The IC_{50} values were determined by nonlinear regression analysis. One-way ANOVA calculated the statistical difference between means with Tukey's multiple comparisons test. All the statistical tests were performed using GraphPad Prism version 8.0.0 for Windows, GraphPad Software, San Diego, California USA, and considered significant when the *p*-value was less than 0.05.

Data availability

All data generated or analyzed during this study are included in this published article (and its ESI†).

Author contributions

Mr Mrugesh Patel and Dr Kaushal Patel conceived and designed the experiments based on the core chemistry, performed the

experiments, analyzed the data, performed the computation work, prepared figures and/or tables, authored and reviewed drafts of the manuscript, and approved the final draft.

Mr Mrugesh Patel, Dr Nilesh Pandey, and Dr Neeraj Jain conceived and designed the experiments based on the core biology, validation of results, prepared figures and/or tables, authored and reviewed manuscript drafts, and approved the final draft.

Dr Alex Chauhan, Mr Paranjay Parikh, and Mr Jignesh Timaniya provided the platform to analyze the data, authored and reviewed drafts of the manuscript, and approved the final draft.

Conflicts of interest

There are no conflicts of interest.

Acknowledgements

The authors express their sincere thanks to the Department of Advanced Organic Chemistry, P. D. Patel Institute of Applied Sciences, Charotar University of Science and Technology (CHARUSAT) for providing research facilities and Dr Franky Shah, Senior Scientific Officer, and Dr Jigna Joshi, Gujarat Cancer and Research Institute, Ahmedabad, India for extending the Cell Analyzer facility.

References

1 H. Sung, J. Ferlay, R. L. Siegel, M. Laversanne, I. Soerjomataram, A. Jemal and F. Bray, *Ca-Cancer J. Clin.*, 2021, **71**, 209–249.
2 D. J. Newman and G. M. Cragg, *J. Nat. Prod.*, 2016, **79**, 629–661.
3 L. Wang, H. L. Wu, X. L. Yin, Y. Hu, H. W. Gu and R. Q. Yu, *Spectrochim. Acta, Part A*, 2017, **170**, 104–110.
4 S. Vilar, E. Quezada, L. Santana, E. Uriarte, M. Yanez, N. Fraiz, C. Alcaide, E. Cano and F. Orallo, *Bioorg. Med. Chem. Lett.*, 2006, **16**, 257–261.
5 K. Venkata Sairam, B. M. Gurupadayya, B. I. Vishwanathan, R. S. Chandan and D. K. Nagesha, *RSC Adv.*, 2016, **6**, 98816–98828.
6 D. A. Ostrov, J. A. Hernández Prada, P. E. Corsino, K. A. Finton, N. Le and T. C. Rowe, *Antimicrob. Agents Chemother.*, 2007, **51**, 3688–3698.
7 Y. Zhang, B. Zou, Z. Chen, Y. Pan, H. Wang, H. Liang and X. Yi, *Bioorg. Med. Chem. Lett.*, 2011, **21**, 6811–6815.
8 M. Curini, F. Epifano, F. Maltese, M. C. Marcotullio, S. P. Gonzales and J. C. Rodriguez, *Aust. J. Chem.*, 2003, **56**, 59–60.
9 A. Manvar, A. Bavishi, A. Radadiya, J. Patel, V. Vora, N. Dodia, K. Rawal and A. Shah, *Bioorg. Med. Chem. Lett.*, 2011, **21**, 4728–4731.
10 L. Zhang, G. Jiang, F. Yao, Y. He, G. Liang, Y. Zhang, B. Hu, Y. Wu, Y. Li and H. Liu, *PLoS One*, 2012, **7**, e37865.
11 R. K. Singh, T. S. Lange, K. K. Kim and L. Brard, *Invest. New Drugs*, 2011, **29**, 63–72.
12 K. V. Sashidhara, S. R. Avula, K. Sharma, G. R. Palnati and S. R. Bathula, *Eur. J. Med. Chem.*, 2013, **60**, 120–127.
13 E. K. Akkol, Y. Genç, B. Karpuz, E. Sobarzo-Sánchez and R. Capasso, *Cancers*, 2020, **12**, 1–25.
14 S. Butler, R. Wang, S. L. Wunder, H. Y. Cheng and C. S. Randall, *Biophys. Chem.*, 2006, **119**, 307–315.
15 A. Zall, D. Kieser, N. Höttecke, E. C. Naumann, B. Thomaszewski, K. Schneider, D. T. Steinbacher, R. Schubenel, S. Masur, K. Baumann and B. Schmidt, *Bioorg. Med. Chem.*, 2011, **19**, 4903–4909.
16 C. Ito, S. Katsuno, M. Itoigawa, N. Ruangrungsi, T. Mukainaka, M. Okuda, Y. Kitagawa, H. Tokuda, H. Nishino and H. Furukawa, *J. Nat. Prod.*, 2000, **63**, 125–128.
17 H. J. Knölker and K. R. Reddy, *Chem. Rev.*, 2002, **102**, 4303–4427.
18 W. Maneerat, T. Ritthiwigrom, S. Cheenpracha, T. Promgool, K. Yossathera, S. Deachathai, W. Phakhodee and S. Laphookhieo, *J. Nat. Prod.*, 2012, **75**, 741–746.
19 X. You, D. Zhu, W. Lu, Y. Sun, S. Qiao, B. Luo, Y. Du, R. Pi, Y. Hu, P. Huang and S. Wen, *RSC Adv.*, 2018, **8**, 17183–17190.
20 S. Issa, A. Prandina, N. Bedel, P. Rongved, S. Yous, M. Le Borgne and Z. Bouaziz, *J. Enzyme Inhib. Med. Chem.*, 2019, **34**, 1321–1346.
21 H. Z. Zhang, Z. L. Zhao and C. H. Zhou, *Eur. J. Med. Chem.*, 2018, **144**, 444–492.
22 A. Ayati, S. Emami, A. Asadipour, A. Shafiee and A. Foroumadi, *Eur. J. Med. Chem.*, 2015, **97**, 699–718.
23 D. Havrylyuk, O. Roman and R. Lesyk, *Eur. J. Med. Chem.*, 2016, **113**, 145–166.
24 P. H. Parikh, J. B. Timaniya, M. J. Patel and K. P. Patel, *Med. Chem. Res.*, 2020, **29**, 538–548.
25 I. M. Khan, M. Islam, S. Shakya, K. Alam, N. Alam and M. Shahid, *Bioorg. Chem.*, 2020, **99**, 103779.
26 A. R. Zabiulla Gulnaz, Y. H. E. Mohammed and S. A. Khanum, *Bioorg. Chem.*, 2019, **92**, 103220.
27 D. C. Liu, M. J. Gao, Q. Huo, T. Ma, Y. Wang and C. Z. Wu, *J. Enzyme Inhib. Med. Chem.*, 2019, **34**, 829–837.
28 K. Karrouchi, S. Radi, Y. Ramli, J. Taoufik, Y. N. Mabkhot, F. A. Al-aizari and M. Ansar, *Molecules*, 2018, **23**, 134.
29 A. Drilon, J. W. Clark, J. Weiss, S.-H. I. Ou, D. R. Camidge, B. J. Solomon, G. A. Otterson, L. C. Villaruz, G. J. Riely, R. S. Heist, M. M. Awad, G. I. Shapiro, M. Satouchi, T. Hida, H. Hayashi, D. A. Murphy, S. C. Wang, S. Li, T. Usari, K. D. Wilner and P. K. Paik, *Nat. Med.*, 2020, **26**, 47–51.
30 A. T. Shaw, G. J. Riely, Y.-J. Bang, D.-W. Kim, D. R. Camidge, B. J. Solomon, M. Varella-Garcia, A. J. Iafrate, G. I. Shapiro, T. Usari, S. C. Wang, K. D. Wilner, J. W. Clark and S.-H. I. Ou, *Ann. Oncol.*, 2019, **30**, 1121–1126.
31 B. J. Solomon, B. Besse, T. M. Bauer, E. Felip, R. A. Soo, D. R. Camidge, R. Chiari, A. Bearz, C.-C. Lin, S. M. Gadgeel, G. J. Riely, E. H. Tan, T. Seto, L. P. James, J. S. Clancy, A. Abbattista, J.-F. Martini, J. Chen, G. Peltz, H. Thurm, S.-H. I. Ou and A. T. Shaw, *Lancet Oncol.*, 2018, **19**, 1654–1667.
32 C. S. Tam, S. Opat, D. Simpson, G. Cull, J. Munoz, T. J. Phillips, W. S. Kim, S. Rule, S. K. Atwal, R. Wei,

W. Novotny, J. Huang, M. Wang and J. Trotman, *Blood Adv.*, 2021, **5**, 2577–2585.
33 G. Ranieri, M. Mammì, E. Donato Di Paola, E. Russo, L. Gallelli, R. Citraro, C. D. Gadaleta, I. Marech, M. Ammendola and G. De Sarro, *Crit. Rev. Oncol. Hematol.*, 2014, **89**, 322–329.
34 K. Nepali, S. Sharma, M. Sharma, P. M. S. Bedi and K. L. Dhar, *Eur. J. Med. Chem.*, 2014, **77**, 422–487.
35 V. G. Bhila, C. V. Patel, N. H. Patel and D. I. Brahmbhatt, *Med. Chem. Res.*, 2013, **22**, 4338–4346.
36 M. Patel and K. Patel, *Heterocycl. Commun.*, 2019, **25**, 146–151.
37 Z. Li and Y. Xing, *Res. Chem. Intermed.*, 2012, **38**, 2223–2228.
38 J. Kapuscinski, *Biotech. Histochem.*, 1995, **70**, 220–233.
39 D. Donjerkovic and D. W. Scott, *Cell Res.*, 2000, **10**, 1–16.
40 S. Cory and J. M. Adams, *Nat. Rev. Cancer*, 2002, **2**, 647–656.
41 W. F. De Azevedo, S. Leclerc, L. Meijer, L. Havlicek, M. Strnad and S. H. Kim, *Eur. J. Biochem.*, 1997, **243**, 518–526.
42 Y.-F. Sun and Y.-P. Cui, *Dyes Pigm.*, 2008, **78**, 65–76.
43 O. Trott and A. J. Olson, *J. Comput. Chem.*, 2009, **31**, 455–461.